Structural diversity and catalytic properties in a family of Ag(I)-benzotriazole based coordination compounds

Article (Accepted Version)

Structural diversity and catalytic properties in a family of Ag(I)-benzotriazole based coordination compounds

Edward Loukopoulos,[a] *Alaa Abdul-Sada,*[a] *Eddy M. E. Viseux,*[a] *Ioannis N. Lykakis*[*b] *and George E. Kostakis**[a]

[a]Department of Chemistry, School of Life Sciences, University of Sussex, Brighton BN1 9QJ, United Kingdom.

E-mail: G.Kostakis@sussex.ac.uk

[b]Department of Chemistry, Aristotle University of Thessaloniki, Thessaloniki 54124, Greece.

E-mail: lykakis@chem.auth.gr

ABSTRACT

In this work we study the coordination chemistry of a series of semi-rigid benzotriazole based ligands (L^1-L^3) along with the low coordination number but versatile Ag^I ions. This has led to nine new coordination compounds formulated $[Ag(L^1)(CF_3CO_2)]$ (**1**), $[Ag_2(L^{1T})_2(CF_3SO_3)_2]\cdot 2Me_2CO$ (**2**), $[Ag(L^{2T})(ClO_4)(Me_2CO)]$ (**3**), $[Ag(L^{2T})(BF_4)(Et_2O)]$ (**4**), $[Ag_2(L^{3T})_2(ClO_4)_2]_2$ (**5**), $[Ag(L^3)(NO_3)]$ (**6**), $[Ag_2(L^{3T})_2(CF_3CO_2)_2]$ (**7**), $[Ag_2(L^{3T})(CF_3SO_3)_2]$ (**8**) and $[Ag_2(L^{3T})_2(CF_3CF_2CO_2)_2]\cdot 2Me_2CO$ (**9**). These compounds show structural diversity including dimers (**5**, **7**, **9**), one dimensional (1D) (**3**, **4**, **6**) and two dimensional (2D) (**1**, **2**, **8**) coordination polymers. The presence of the two $-CH_2-$ units between the three rigid backbones, benzotriazole/$-C_6H_4-$/benzotriazole, provides a limited, but significant, flexibility in L^1-L^3, influencing their variety coordination abilities. Interestingly, certain structures exhibit an isomerism effect (L^{1T}-L^{3T}) in the benzotriazole unit when in solid state; a series of studies are indicative of the 1,1- form is generally dominant in solution even in cases where the crystal structure does not contain this tautomer. The homogeneous catalytic efficacy of all compounds against the well-known multi component A^3 coupling reaction and the hydration of alkynes were investigated. Compound **4** was identified as the optimal catalyst for both reactions, promoting the multicomponent coupling as well as the alkyne hydration reaction under low loadings (0.5 and 3 mol%, respectively) and in high yields (up to 99 and 93% in each case).

INTRODUCTION

The induction of the crystal engineering concept[1] in coordination chemistry has led to the rational design of many novel coordination polymers (CPs) and metal organic frameworks (MOFs) with interesting properties. One of the most promising application of these materials is catalysis. In this context, the chosen systems may be highly tunable due to the many possible combinations of chemical (metal selection, coordination environment and geometry, ligand selection) and synthetic (e.g. solvent, metal(s)-ligand(s) ratio, temperature) parameters, allowing for greater understanding and control of the procedure. Since the first reports[2,3] that utilized these concepts, efforts have intensified with various one-[4,5], two-[6–10] and three-dimensional coordination polymers[11–13] being used as catalysts in a variety of reactions.

In regards to the metal selection for the construction of these coordination architectures, Ag has been receiving increasing attention due to its rich and unique chemistry. Compared to other metals, Ag^{I} provides a wide range of coordination environments, with multiple possibilities in coordination number (from 2 to 6) and geometries (e.g. linear, trigonal, tetrahedral, trigonal bipyramidal, square pyramidal, octahedral)[14]. This versatility and adaptability of Ag^{I} systems, along with the potential formation of argentophilic (Ag^{I} – Ag^{I}) interactions, has contributed significantly to the formation of peculiar structural topologies[15–24] with various dimensionalities, as well as uncommon supramolecular architectures[25]. These exploits have also been crucial towards the development of Ag^{I} coordination polymers with structural interest and potential applications, which include luminescence[26–28], anion exchange[28–30], antibacterial[31–37] and catalytic activity.[38–44] Focusing on the latter, several Ag CPs and MOFs have been especially used as catalysts in organic transformations that involve alkyne activation[45,46] due to the supreme capability of the metal to form organometallic intermediates through π-coordination with the carbon–carbon triple bond.

Our group has had a long-standing interest in coordination compounds derived from semi-rigid organic ligands, especially N-donors. As a part of this, in previous works we investigated the transition metal chemistry of semi-rigid benzotriazole-based ligands L^1-L^3 (Scheme 1), focusing on the relevant Co and Cu systems[47–50]. The results demonstrated the rich chemistry and flexibility of these N-containing ligands. Optimization of the system in these studies led to multiple coordination compounds and low dimensional CPs with interesting magnetic and catalytic properties, which were largely dependent on the unique effects of the benzotriazole units in the coordination environment.

The next step in our studies was to combine this rewarding and flexible system with the rich chemistry and unique coordination variety of Ag^I ions, exploring the resulting structural aspects as well as potential catalytic applications to add to our existing findings. Having the superior alkynophilicity of Ag^I in mind, we identified the A^3 multicomponent coupling and the hydration of terminal alkynes as two potential reactions to test any afforded compounds. The former reaction involves a coupling between an aldehyde, an amine and an alkyne to generate propargylamines; these molecules are of significant importance in synthetic chemistry, acting as intermediates towards biologically active compounds as well as natural products[51–54]. The key mechanistic step during this reaction requires the formation of a metal acetylide intermediate which is then added to the iminium ion. For this reason, a variety of Ag^I sources has been utilized in this reaction,[55] including simple salts[56], coordination compounds[57–60] and CPs[41,42,61]. The second reaction involves treatment of alkynes with water, resulting to the synthesis of ketones that follow Markonikov's rule. As the classic method for this reaction requires the addition of toxic mercury under harsh acidic conditions, multiple systems involving other transition metal elements (e.g Cu[62], Fe[63], Ru[64], Au[65]) have also been explored. Another common strategy[66–68] involves incorporation of silver as a co-catalyst with gold to activate this reaction; on the other hand, only a few reports using solely silver sources as

catalysts can be found. The first example dates back to 2012, when Wagner and co-workers[69] employed $AgSbF_6$ for the selective hydration of terminal alkynes. In the following years $AgBF_4$[70], AgOTf[71] and a silver exchanged silicotungstic acid (STA) catalyst[72] were also tested successfully. However considerable disadvantages in these procedures, such as the high loadings (up to 10 mol% in most cases) or temperatures, the use of expensive salts (such as $AgSbF_6$) or the lengthy workup for the preparation of the catalyst (in the case of AgSTA) reveal the need for further optimization in this area. In addition, no silver coordination compounds have been reported to catalyze this reaction up to this date to the best of our knowledge.

As a result of all the above, herein we report on two subsequently (interconnected) subjects i) the synthesis and characterization of compounds $[Ag(L^1)(CF_3CO_2)]$ (**1**), $[Ag_2(L^{1T})_2(CF_3SO_3)_2]\cdot 2Me_2CO$ (**2**), $[Ag(L^{2T})(ClO_4)(Me_2CO)]$ (**3**), $[Ag(L^{2T})(BF_4)(Et_2O)]$ (**4**), $[Ag_2(L^{3T})_2(ClO_4)_2]_2$ (**5**), $[Ag(L^3)(NO_3)]$ (**6**), $[Ag_2(L^{3T})_2(CF_3CO_2)_2]$ (**7**), $[Ag_2(L^{3T})(CF_3SO_3)_2]$ (**8**) and $[Ag_2(L^{3T})_2(CF_3CF_2CO_2)_2]\cdot 2Me_2CO$ (**9**) and ii) the demonstration of the catalytic activity of these compounds in the A^3 coupling and alkyne hydration reactions.

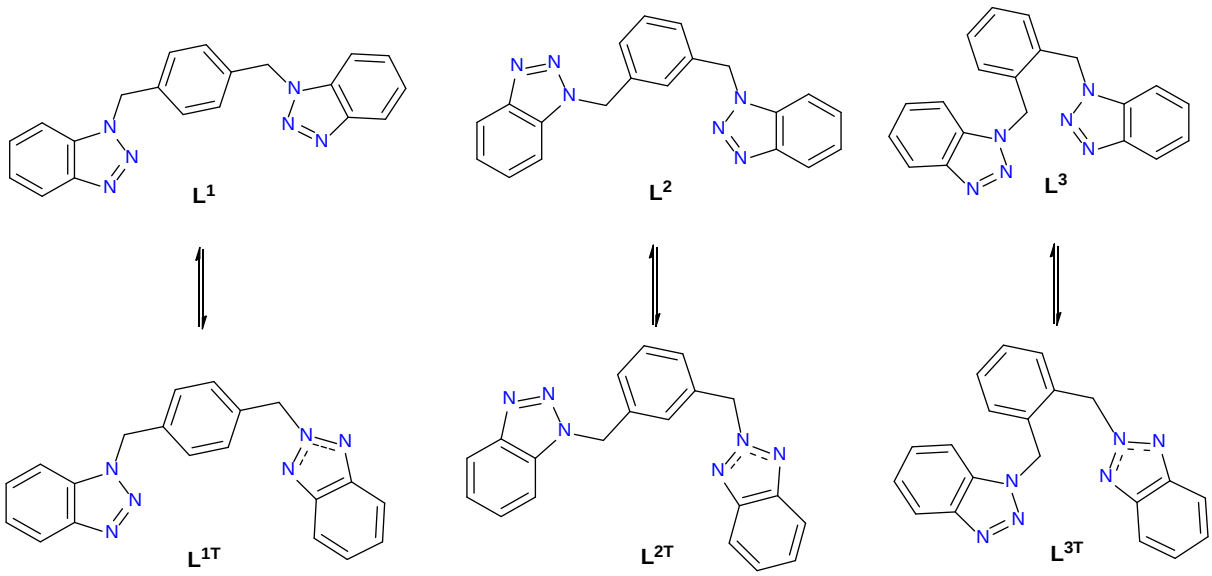

Scheme 1. The organic ligands L^1, L^2, and L^3 used in this study.

EXPERIMENTAL

Materials. Chemicals (reagent grade) were purchased from Sigma Aldrich, Acros Organics and Alfa Aesar. Materials and solvents were used with no further purification. Ligands L^1– L^3 were synthesized according to the reported procedure[47]. *Safety note*: Perchlorate salts are potentially explosive; such compounds should be used in small quantities and handled with caution and utmost care at all times. All crystallization experiments were performed in the absence of light, although the resulting silver compounds do not appear to be light sensitive.

Instrumentation. IR spectra of the samples were recorded over the range of 4000-650 cm^{-1} on a Perkin Elmer Spectrum One FT-IR spectrometer fitted with a UATR polarization accessory. EI-MS was performed on a VG Autospec Fissions instrument (EI at 70 eV). TGA analysis was performed on a TA Instruments Q-50 model (TA, Surrey, UK) under nitrogen and at a scan rate of 10°C/min. NMR spectra were measured on a Varian VNMRS solution-state spectrometer at 30°C. Chemical shifts are quoted in parts per million (ppm). Coupling constants (J) are recorded in Hertz (Hz).

X-Ray crystallography. Data for **L^1** and compounds **1**-**5**, **8** were collected (ω-scans) at the University of Sussex, using either a Rigaku 007HF rotating anode generator with CCD plate detector (for **L^1**, **1**, **2**) or an Agilent Xcalibur Eos Gemini Ultra diffractometer with CCD plate detector (for **3**-**5**, **8**), under a flow of nitrogen gas at 173(2) K and Mo Kα (λ = 0.71073 Å) or Cu Kα radiation (λ = 1.54184 Å). CRYSALIS CCD and RED software was used respectively for data collection and processing. Reflection intensities were corrected for absorption by the multi-scan method. Data for **6**, **7** and **9** were collected at the National Crystallography Service, University of Southampton.[73] All structures were determined using Olex2[74], solved using SHELXT[75,76] and refined with SHELXL-2014[77]. All non-H atoms were refined with anisotropic thermal parameters, and H-atoms were introduced at calculated positions and allowed to ride on their carrier atoms. Crystal data and structure refinement parameters for

these compounds are given in Tables S1-S2. Geometric/crystallographic calculations were performed using PLATON[78], Olex2[74], and WINGX[77] packages; graphics were prepared with Crystal Maker and MERCURY[79]. Each of the crystal structures has been deposited at the CCDC 1851153-1851162.

SYNTHETIC PROCEDURES

General catalytic protocol for A^3 coupling. A mixture of aldehyde (1 mmol), amine (1.1 mmol), alkyne (1.3 mmol), Ag catalyst (ca. 3 mg, 0.5 mol%, based on the aldehyde amount) and 2-propanol (5 ml) was added into a sealed tube and stirred at 90 °C for appropriate time. After completion of the reaction, the mixture was left to cool to room temperature, filtered upon a short pad of silica (to separate the catalyst) and the filtrate was evaporated under vacuum. The corresponding propargyl amine was isolated in pure form by column chromatography using silica gel and a solvent mixture of hexane/EtOAc in a ratio from 10/1 to 5/1 as the eluent. The characterization data of the products matched well with those reported in the literature[49].

General catalytic protocol for alkyne hydration. A mixture of alkyne (1 mmol), water (150 μl), Ag catalyst (18 mg, 3 mol%, based on the alkyne amount) and methanol (1.5 ml) was added into a sealed tube and stirred at 90 °C for 24 hr. The mixture was then allowed to cool to room temperature and filtered upon a short pad of silica (to withhold the catalyst). The resulting residue was then loaded to a flash column chromatography using silica gel and the corresponding ketone was isolated in pure form using a mixture of hexane/EtOAc in a ratio from 10/1 to 3/1, as the eluent.

Synthesis of $[Ag(L^1)(CF_3CO_2)]$ (**1**). 0.06 mmol (0.020 g) of L^1 were dissolved in 17.5 ml MeCN while stirring to produce a colorless solution. 0.12 mmol (0.027 g) of $AgCF_3CO_2$ were then added and the resulting white solution was filtrated and left undisturbed under room temperature to produce white needles after 12 days. Selected IR peaks (cm^{-1}): 3098 (w), 1691

(w), 1593 (w), 1497 (w), 1454 (w), 1310 (w), 1278 (w), 1226 (m), 1162 (w), 1114 (m), 1033 (m), 825 (w), 780 (m), 738 (s), 621 (w). Yield: 36% (based on Ag).^{1}H NMR (600 MHz, DMSO-d_6) δ 8.02 (d, J = 8.3 Hz, 2H), 7.78 (d, J = 8.4 Hz, 2H), 7.49 (t, J = 7.7 Hz, 2H), 7.37 (d, J = 7.8 Hz, 2H), 7.29 (s, 4H), 5.93 (s, 4H). Elemental Analysis for $C_{22}H_{16}AgF_3N_6O_2$: C 47.08, H 2.87, N 14.97; found C 47.01, H 2.81, N 15.08.

Synthesis of $[Ag_2(L^{1T})_2(CF_3SO_3)_2]\cdot 2Me_2CO$ (**2**). 0.06 mmol (0.020 g) of L^1 were dissolved in 17.5 ml Me_2CO while stirring to produce a colorless solution. 0.12 mmol (0.031 g) of AgOTf were then added. The resulting white solution was filtrated, then layered over n-hexane in a 1:2 ratio. White needles were obtained after 8 days. Selected IR peaks (cm^{-1}): 3404 (w), 1705 (w), 1574 (m), 1517 (w), 1421 (w), 1285 (m), 1234 (m), 1160 (m), 1026 (s), 866 (w), 795 (w), 747 (s), 635 (s). Yield: 32% (based on Ag).^{1}H NMR (600 MHz, DMSO-d_6) δ 8.03 (d, *J* = 8.0 Hz, 2H), 7.80 (d, *J* = 8.3 Hz, 2H), 7.50 (t, *J* = 7.2 Hz, 2H), 7.38 (t, *J* = 7.0 Hz, 2H), 7.30 (s, 4H), 5.94 (s, 4H). Elemental Analysis for $C_{48}H_{44}Ag_2F_6N_{12}O_8S_2$: C 43.98, H 3.38, N 12.82; found C 44.11, H 3.30, N 12.85.

Synthesis of $[Ag(L^{2T})(ClO_4)(Me_2CO)]$ (**3**). 0.12 mmol (0.041 g) of L^2 were dissolved in 10 ml Me_2CO while stirring to produce a colorless solution. A solution containing 0.12 mmol (0.027 g) of $AgClO_4$ in Me_2CO (10 ml) was slowly added. The resulting white solution was filtrated, then layered over Et_2O in a 1:2 ratio. White needles were obtained after 4 days. Selected IR peaks (cm^{-1}): 1689 (m), 1594 (w), 1496 (w), 1455 (m), 1318 (m), 1286 (m), 1226 (m), 1159 (w), 1084 (s), 818 (w), 780 (m), 750 (s), 622 (s). Yield: 81% (based on Ag).^{1}H NMR (600 MHz, DMSO-d_6) δ 8.02 (d, *J* = 8.4 Hz, 2H), 7.72 (d, *J* = 8.2 Hz, 2H), 7.46 (t, *J* = 7.5 Hz, 2H), 7.37 (dd, *J* = 16.6, 9.5 Hz, 3H), 7.31 (t, *J* = 7.6 Hz, 1H), 7.24 (d, *J* = 7.7 Hz, 2H), 5.94 (s, 4H). Elemental Analysis for $C_{23}H_{22}AgClN_6O_5$: C 44.60, H 3.86, N 13.87; found C 44.44, H 3.65, N 14.05.

Synthesis of [$Ag(L^{2T})(BF_4)(Et_2O)$] (**4**). **4** was synthesized using the same method and ratios as **3**, with $AgBF_4$ (0.023 g) as the metal salt. White needles were obtained after 3 days. Selected IR peaks (cm^{-1}): 3098 (w), 1593 (w), 1497 (w), 1456 (w), 1310 (w), 1287 (w), 1226 (m), 1157 (w), 1055 (s), 1034 (s), 818 (w), 779 (m), 751 (s), 741 (s), 698 (w), 640 (w), 618 (w). Yield: 79% (based on Ag). ^{1}H NMR (600 MHz, DMSO-d_6) δ 8.04 (d, J = 8.3 Hz, 2H), 7.73 (d, J = 8.3 Hz, 2H), 7.47 (t, J = 7.6 Hz, 2H), 7.38 (dd, J = 16.0, 8.9 Hz, 3H), 7.33 (t, J = 7.6 Hz, 1H), 7.25 (d, J = 7.5 Hz, 2H), 5.95 (s, 4H). ^{15}N NMR (40 MHz, DMSO-d_6) δ -155.99. Elemental Analysis for $C_{24}H_{26}AgBF_4N_6O$: C 47.32, H 4.30, N 13.80; found C 44.59, H 3.70, N 12.87. This result corresponds to the presence of two water molecules. Elemental Analysis for $(C_{24}H_{26}AgBF_4N_6O)(H_2O)_2$: C 44.68, H 3.69, N 13.03.

Synthesis of $[Ag_2(L^{3T})_2(ClO_4)_2]_2$ (**5**). 0.12 mmol (0.041 g) of L^3 were dissolved in 10 ml Me_2CO while stirring to produce a colorless solution. A solution containing 0.12 mmol (0.027 g) of $AgClO_4$ in Me_2CO (10 ml) was slowly added. The resulting white solution was filtrated, then left undisturbed under room temperature to produce white needles after 2 days. Selected IR peaks (cm^{-1}): 1705 (w), 1594 (w), 1497 (w), 1457 (m), 1226 (m), 1153 (m), 1087 (s), 1025 (m), 953 (w), 856 (w), 780 (m), 765 (m), 741 (s), 622 (s). Yield: 88% (based on Ag).^{1}H NMR (500 MHz, DMSO-d_6) δ 8.04 (d, J = 8.3 Hz, 2H), 7.88 (dd, J = 6.6, 3.2 Hz, 4H), 7.71 (d, J = 8.4 Hz, 2H), 7.50 (t, J = 7.7 Hz, 2H), 7.45 – 7.37 (m, 6H), 7.36 – 7.20 (m, 6H), 6.98 (d, J = 7.3 Hz, 2H), 6.24 (d, J = 4.8 Hz, 8H). These shifts indicate the presence of both isomer forms (1,1 and 1,2) in a 1:1 ratio. Elemental Analysis for $C_{40}H_{32}Ag_2Cl_2N_{12}O_8$: C 43.86, H 2.94, N 13.34; found C 43.78, H 2.85, N 13.37.

Synthesis of [$Ag(L^3)(NO_3)$] (**6**). 0.06 mmol (0.020 g) of L^3 were dissolved in 10 ml MeCN while stirring to produce a colorless solution. After five minutes a solution containing 0.12 mmol (0.020 g) of $AgNO_3$ in MeCN (10 ml) was slowly added. The resulting white solution was filtrated, then layered over Et_2O in a 1:2 ratio. Colorless blocks were obtained after 1 day.

Selected IR peaks (cm^{-1}): 1592 (w), 1495 (w), 1455 (m), 1413 (m), 1290 (m), 1228 (m), 1161 (m), 1135 (w), 1113 (w), 1087 (w), 1033 (w), 1001 (w), 958 (w), 885 (w), 842 (w), 818 (w), 767 (m), 759 (m), 748 (s), 708 (w), 667 (w), 625 (w). Yield: 82% (based on Ag).^{1}H NMR (399 MHz, DMSO-d_6) δ 8.09 (d, J = 8.4 Hz, 2H), 7.78 (d, J = 8.3 Hz, 2H), 7.54 (t, J = 7.6 Hz, 2H), 7.44 (t, J = 7.5 Hz, 2H), 7.28 – 7.21 (m, 2H), 6.96 – 6.89 (m, 2H), 6.27 (s, 4H). ^{15}N NMR (40 MHz, DMSO-d_6) δ -154.37. Elemental Analysis for $C_{20}H_{16}AgN_7O_3$: C 47.08, H 3.16, N 19.22; found C 47.18, H 3.25, N 19.33.

Synthesis of $[Ag_2(L^{3T})_2(CF_3CO_2)_2]$ (**7**). 0.06 mmol (0.020 g) of L^3 were dissolved in 10 ml Me_2CO while stirring to produce a colorless solution. A solution containing 0.12 mmol (0.027 g) of $AgCF_3CO_2$ in Me_2CO (10 ml) was slowly added. The resulting white solution was filtrated, then layered over n-hexane in a 1:2 ratio. White needles were obtained after 2 days. Selected IR peaks (cm^{-1}): 1665 (w), 1595 (w), 1499 (w), 1457 (m), 1222 (s), 1147 (s), 1025 (s), 952 (w), 837 (w), 780 (m), 746 (s), 633 (s). Yield: 52% (based on Ag).^{1}H NMR (600 MHz, DMSO-d_6) δ 8.09 (d, J = 8.5 Hz, 1H), 8.06 (d, J = 8.6 Hz, 1H), 7.92 – 7.86 (m, 2H), 7.79 (d, J = 8.4 Hz, 1H), 7.75 (d, J = 8.4 Hz, 1H), 7.57 – 7.48 (m, 3H), 7.46 – 7.37 (m, 5H), 7.34 – 7.21 (m, 5H), 6.97 (d, J = 7.5 Hz, 1H), 6.94 – 6.89 (m, 2H), 6.28 –6.26 (m, 8H). These shifts indicate the presence of both isomer forms (1,1 and 1,2) in a 1:1 ratio. Elemental Analysis for $C_{44}H_{32}Ag_2F_6N_{12}O_4$: C 47.08, H 2.87, N 14.97; found C 47.00, H 2.84, N 15.06.

Synthesis of $[Ag_2(L^{3T})(CF_3SO_3)_2]$ (**8**). A procedure similar to the synthesis of **7** was followed, using AgOTf (0.12 mmol, 0.031 g) as the metal salt. White needles were obtained after 1 day. Selected IR peaks (cm^{-1}): 1594 (w), 1498 (w), 1458 (m), 1265 (s), 1241 (s), 1223 (s), 1166 (m), 1023 (s), 956 (w), 861 (w), 766 (w), 751 (s), 740 (s), 629 (s), 606 (w). Yield: 58% (based on Ag).^{1}H NMR (600 MHz, DMSO-d_6) δ 8.08 (d, J = 8.4 Hz, 2H), 8.05 (d, J = 8.4 Hz, 1H), 7.90 – 7.85 (m, 2H), 7.79 (d, J = 8.4 Hz, 2H), 7.76 (d, J = 8.4 Hz, 1H), 7.58 – 7.49 (m, 3H), 7.46 – 7.38 (m, 3H), 7.34 – 7.21 (m, 3H), 6.99 (d, J = 7.5 Hz, 1H), 6.94 (dd, J = 5.6, 3.5 Hz, 2H), 6.27

(s, 6H). These shifts indicate the presence of both isomer forms (1,1 and 1,2) in a 2:1 ratio. Elemental Analysis for $C_{22}H_{16}Ag_2F_6N_6O_6S_2$: C 30.93, H 1.89, N 9.84; found C 31.10, H 2.01, N 9.86.

Synthesis of $[Ag_2(L^{3T})_2(CF_3CF_2CO_2)_2]\cdot 2Me_2CO$(**9**). A procedure similar to the synthesis of **7** was followed, using $AgCF_3CF_2CO_2$ (0.12 mmol, 0.033 g) as the metal salt. White needles were obtained after 3 days. Selected IR peaks (cm^{-1}):1661 (m), 1499 (w), 1455 (w), 1319 (m), 1277 (w), 1212 (m), 1166 (m), 1147 (m), 1022 (m), 852 (w), 815 (w), 771 (w), 747 (s), 728 (s), 628 (w). Yield: 64% (based on Ag).^{1}H NMR (600 MHz, DMSO-d_6) δ 8.05 (d, J = 8.4 Hz, 2H), 7.90 (dd, J = 6.6, 3.1 Hz, 4H), 7.74 (d, J = 8.4 Hz, 2H), 7.50 (t, J = 7.7 Hz, 2H), 7.43 (dd, J = 6.6, 3.0 Hz, 4H), 7.39 (t, J = 7.7 Hz, 2H), 7.34 – 7.20 (m, 6H), 6.95 (d, J = 7.5 Hz, 2H), 6.28 (s, 4H), 6.26 (s, 4H). These shifts indicate the presence of both isomer forms (1,1 and 1,2) in a 1:1 ratio. Elemental Analysis for $C_{49}H_{38}Ag_2F_{10}N_{12}O_5$: C 45.96, H 2.99, N 13.12; found C 45.97, H 3.06, N 13.20.

CRYSTAL STRUCTURE DESCRIPTION

Compound **1** was synthesized using silver trifluoroacetate and the *para*-substituted L^1 ligand. The structure crystallizes in the triclinic $P\bar{1}$ space group and its asymmetric unit consists of one Ag^I center, one L^1 molecule and one trifluoroacetate anion. In this coordination mode, L^1 adopts a chair conformation, with the benzotriazole units being parallel to each other. Each ligand molecule coordinates to a total of two Ag^I centers as seen in Scheme 2, mode A. The trifluoroacetate anions also act as bridging ligands, generating $[Ag_2(L^1)_4(CF_3CO_2)_2]$ nodes which expand to a two dimensional architecture. As a result, **1** may be described as a 2D coordination polymer that propagates along the *a0c* plane (Figure 1, left). Each of the metal centers possesses a tetrahedral geometry and a $\{N_2O_2\}$ coordination environment. This tetrahedron is rather distorted, with the relevant angles ranging from 97.18(18) to 140.94(19)°.

The related Ag-N and Ag-O bond distances are surprisingly similar, ranging from 2.304(5) to 2.340(5) Å. No hydrogen bonds or other supramolecular interactions were observed.

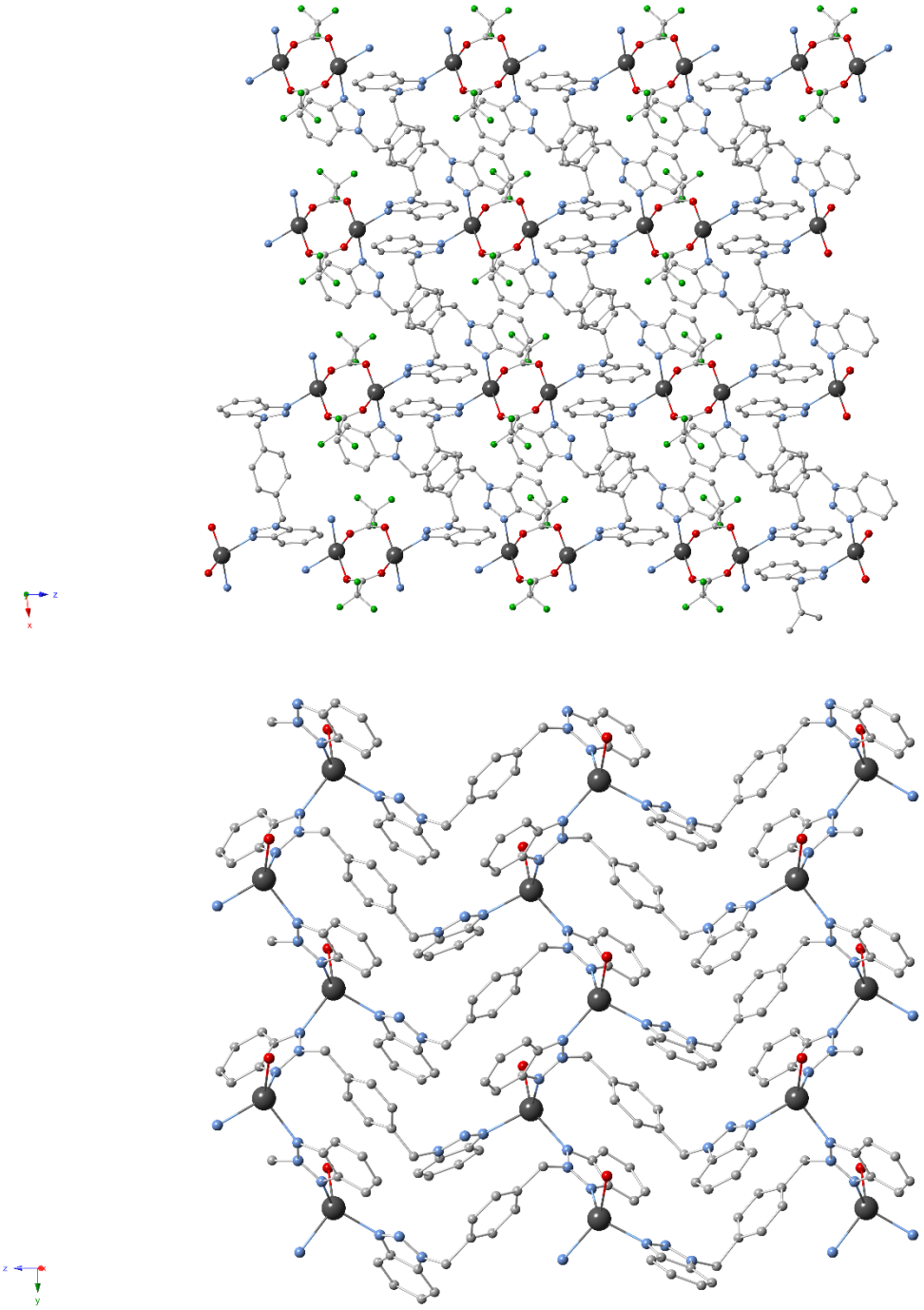

Figure 1. (up) Part of the two-dimensional framework along the *a0c* plane in compound **1**. H atoms are omitted for clarity. (down) Part of the two-dimensional framework along the *b0c*

plane in compound **2**. For clarity, H atoms, solvent molecules and part of the triflate anions have been omitted. Color code Ag (anthracite), C (light grey), N (light blue), O (red), F (light green).

Compound **2** was synthesized through the use of silver triflate as the metal salt and the resulting structure crystallizes in the monoclinic $P2_1$ space group. In this case, an isomerism phenomenon is observed in the benzotriazole moieties of all L^1 molecules, as one of the two $-CH_2$ linkers connects to the middle N atom of the benzotriazole. Consequently, the disubstituted 1,2-yl analogue (L^{1T}) is obtained, instead of the 1,1-yl. As a result the asymmetric unit of **2** contains two Ag^I centers, two L^{1T} molecules, two triflate anion molecules that act as terminal ligands and two acetone lattice solvents. The latter will not be further mentioned in this description. The coordination mode for the two crystallographically independent L^{1T} molecules (Scheme 2, Modes B and C) is similar, as each of the ligands coordinates to three different Ag^I centers. More specifically, the benzotriazol-1-yl unit coordinates to one Ag^I center through the single far nitrogen atom, while the 2-yl moiety coordinates to two metal centers through its two far nitrogen atoms. The two L^{1T} molecules however differ slightly in orientation as the angle between their benzotriazole entities are 49.27(3) and 43.47(3)° respectively. This conformation accounts for the formation of $[Ag_2(L^{1T})_2(CF_3SO_3)_2]$ nodes which are connected to each other through Ag-N bonding to generate the resulting two-dimensional coordination polymer along the *b0c* plane (Figure 1, right). Each Ag^I center possesses a $\{N_3O\}$ coordination environment and a slightly distorted tetrahedral geometry. The Ag-N bonds range from 2.266(10) to 2.349(10) Å, while the Ag-O are slightly larger at 2.323(15) and 2.366(9) Å. The angles of the tetrahedra range from 97.2(3) to 135.0(3)°. While no strong H-bonds are formed, π···π interactions form between the benzene and the

benzotriazole moieties of ligand molecules to further stabilize the two dimensional architecture. The parameters for these interactions are detailed in Table S3.

For the construction of compound **3** the meta-substituted ligand L^2 was utilized along with silver perchlorate. The complex crystallizes in the monoclinic $P2_1/n$ space group and contains one Ag^I center, a ligand molecule, a perchlorate anion as well as one acetone molecule in the asymmetric unit. Interestingly, another case of ligand isomerism is observed as the ligand molecule appears as the 1,2-disubstituted benzotriazole analogue (L^{2T}). Each of these L^{2T} ligands coordinates to two different Ag^I centers through the far N atom of each benzotriazole moiety. Due to the increased flexibility of the $–CH_2$ linkers, in this conformation mode (Scheme 2, Mode D) the planes of the two benzotriazole moieties are found at an angle of 54.56(19)°. As a result of these features, the structure of **3** consists of a one-dimensional polymeric chain which propagates along the *b* axis (Figure 2, upper). The perchlorate and acetone molecules also coordinate to the Ag^I center, which exhibits a heavily distorted tetrahedral geometry in a $\{N_2O_2\}$ coordination environment. As expected, the Ag-O bond distances, ranging from 2.47520(8) to 2.52007(9) Å, are significantly larger than the analogous Ag-N values which were calculated at 2.15565(8) and 2.18819(7) Å respectively.

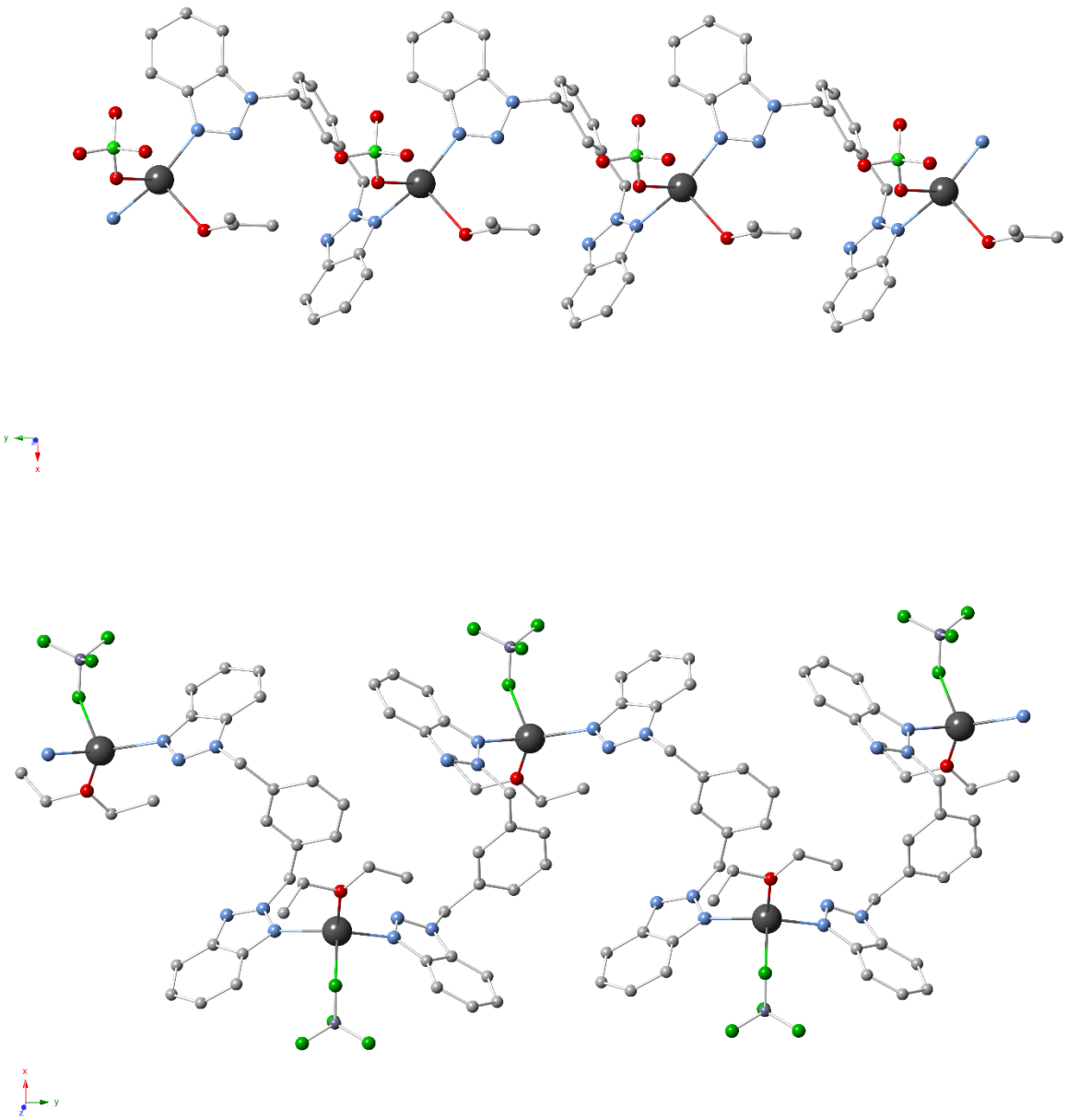

Figure 2. (up) Part of the one-dimensional framework in **3**. H atoms are omitted for clarity. (down) Part of the one-dimensional framework in **4** along the *b* axis. H atoms are omitted for clarity. Color code Ag (anthracite), C (light grey), N (light blue), B (dark grey), F/Cl (light green).

Compound **4** was found to crystallize in the monoclinic $P2_1/n$ space group. Determination of the structure through X-Ray crystallography reveals a similar case of isomerization of L^2 to L^{2T} as seen in **3**. However, in this case the ligand shows a different conformation (Scheme 2, Mode E), as the two benzotriazole moieties are almost parallel to each other at an angle of only 3.70(11)°. Due to this, the compound propagates in one direction, forming 1D helix-like chains along the *b* axis as shown in Figure 2, lower. This difference in the conformation of L^{2T} also accounts for significant variance in Ag-Ag distance; this value was measured at 8.9893(4) Å in **3** and 10.3143(9) Å in **4**. Each Ag^I center is coordinated to four atoms in a distorted tetrahedral geometry. The coordination environment consists of two N atoms from two L^{2T} molecules, one F atom from tetrafluoroborate anions and one O atom from a coordinating diethyl ether solvent molecule. The largest bond in this coordination sphere is the Ag-F distance which was measured at 2.615(4) Å. In contrast, the Ag-N bond values were the smallest at 2.224(5) and 2.250(4) Å. The arrangement of the framework also promotes the formation of inter-molecular $\pi\cdots\pi$ interactions which account for further stability.[80] These weak interactions occur between certain benzotriazole aromatic rings, as detailed in Table S4.

Compound **5** crystallizes in the triclinic $P\bar{1}$ space group and its structure consists of two crystallographically independent dimeric $[Ag_2(L^{3T})_2(ClO_4)_2]$ units as shown in Figure 3. Similarly to the *para*- and *meta*- analogues, the *ortho*-substituted ligand also appears here as the L^{3T} isomer. The presence of two different types of dimeric units within the structure are due to the coordination modes and conformations of L^{3T} (Scheme 2, Modes F and G). In the first unit the benzotriazol-1-yl moiety coordinates to both Ag^I centers through the respective middle and far nitrogen atoms; the related atoms appear aligned in a single plane. The 2-yl moiety is found at an angle of 63.31(9)° to this plane and coordinates to only one metal center. As a result, the relevant Ag^I centers possess a distorted tetrahedral $\{N_3O\}$ environment. In contrast, the second dimer consists of L^{3T} ligands in which the benzotriazole entities are almost parallel

(6.02(8)° angle between the two planes). This dimeric component is further stabilized by a weak Ag···π interaction which is formed as the phenyl group of the ligand backbone faces towards the silver atom with a slight slippage of 1.717 Å, as depicted in Scheme S1. The centroid-metal distance in this case was measured at 3.177(2) Å. A series of relevant Ag···C distances from 2.737(5) to 3.317(5) further support the formation of this interaction. Each of these units coordinate to one Ag^{I} center through their respective far nitrogen atoms and therefore the metal ions show a distorted trigonal geometry and a $\{N_2O\}$ coordination environment. The formation of several intermolecular π···π interactions (Table S5) further stabilizes the packing arrangement of these dimeric units.

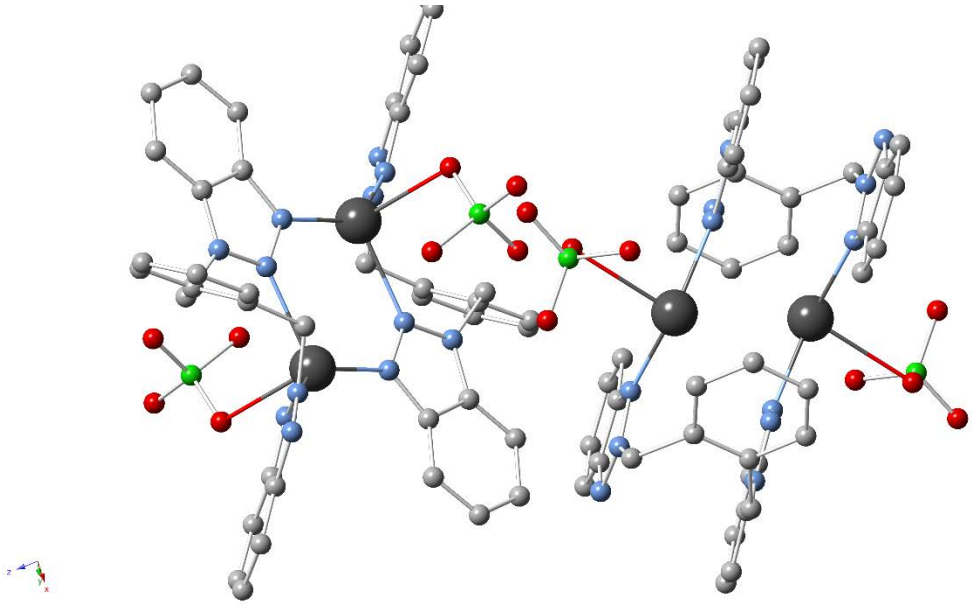

Figure 3. The two crystallographically independent dimeric units in **5**. H atoms are omitted for clarity. Color code Ag (anthracite), C (light grey), N (light blue), O (red), Cl (light green).

Crystallographic analysis for compound **6** reveals a one-dimensional polymeric structure which extends along the *b* axis to form a ribbon-like 1D framework with small voids (Figure4, left). The compound crystallizes in the triclinic $P\bar{1}$ space group and its asymmetric unit contains an Ag^{I} center, one L^{3} ligand molecule and one nitrate anion which acts as a

bridging ligand. Interestingly, no isomerization of the ligand is observed: each of the benzotriazol-1-yl moieties coordinate to one Ag^{I} ion through the far nitrogen atom (Scheme 2, Mode H), with the respective Ag-Ag distance at 10.749(3) Å. In regards to the ligated nitrate anion, one oxygen atom coordinates to the metal ion, while another oxygen coordinates to the same Ag^{I} center as well as a symmetry related one. As a result, two zig-zag 1D architectures are bridged by the nitrate anions to form the resulting ribbon-like framework. The resulting $\{N_2O_3\}$ coordination environment of the metal ion provides a distorted square pyramidal geometry ($\tau = 0.05$[81]). As expected, the mean Ag-N distances (2.242(7) and 2.243(6) Å) are significantly shorter than the respective Ag-O distances (ranging from 2.512(6) to 2.720(6) Å).

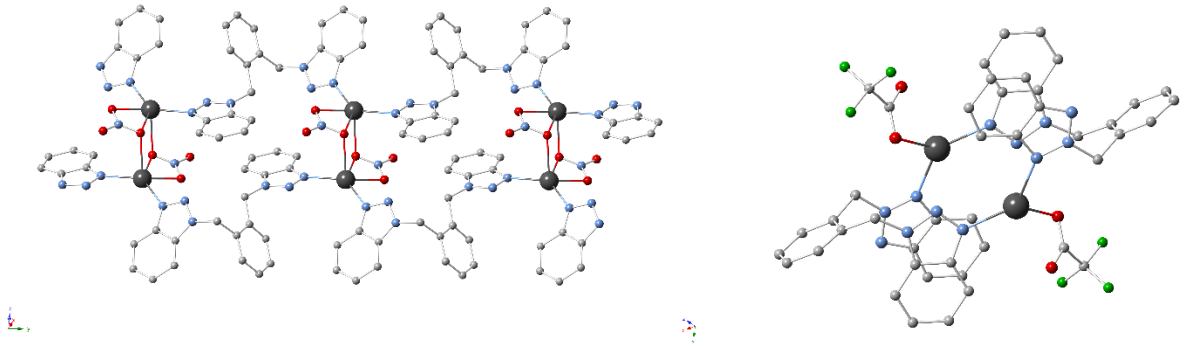

Figure 4. (left) Part of the one-dimensional framework in **6** along the *b* axis. H atoms are omitted for clarity. Color code Ag (anthracite), C (light grey), N (light blue), O (red). (right) The structure of compound **7**. H atoms are omitted for clarity. Color code Ag (anthracite), C (light grey), N (light blue), O (red), F (green).

Compounds **7** and **9** contain isoskeletal cores and as such only the former will be described in detail. The structure of **7** consists of a wheel-like $[Ag_2(L^{3T})_2(CF_3CO_2)_2]$ dimeric unit in which the ligand appears as the L^{3T} isomer (Figure 4, right). Similarly to one of the dimers in compound **5**, the benzotriazole moieties in the ligand are found almost parallel to each other at an angle of 7.97(8)° and coordinate to a total of two Ag^{I} ions through their

respective far nitrogen atoms(Scheme 2, Mode I). This Ag-Ag distance was measured at 3.9108(7) Å. A trifluoroacetate anion also coordinates to the metal center through one oxygen atom to complete its $\{N_2O\}$ coordination sphere. The relevant angles in this trigonal geometry range from 105.18(13)° to 127.82(11)°. Intermolecular π···π interactions provide extended stability to this architecture. The parameters for these interactions may be found at Table S6.

Finally, compound **8** crystallizes in the monoclinic $P2_1/n$ space group and its asymmetric unit contains two Ag^I centers, two triflate anion molecules and one organic ligand as the L^{3T} isomer. The conformation of the latter is similar to other compounds mentioned in this study, with the planes of the benzotriazole entities forming a very small angle of 12.18(12)°. However, the coordination mode varies in this case, as the benzotriazol-2-yl unit utilize both far nitrogen atoms to coordinate to two metal centers (Scheme 2, Mode J). The ligated triflates also play an important role in the resulting architecture as they bridge symmetry related $[Ag_2(L^{3T})_2]$ nodes. This bridging leads to the formation of a two-dimensional sheet along the *b0c* plane (Figure 5) which is supported by argentophilic interactions between two symmetry-related Ag^I centers which are found at a distance of 3.1794(11) Å. Further support is provided by the formation of week π···π interactions between aromatic rings as detailed in Table S7.It is worth noting that each of the triflate units bridge the aforementioned nodes in a different way (Scheme 2, bottom middle and right). For the first triflate, each of the three oxygen atoms coordinate to different Ag^I ions, while the second anion employs only one oxygen atom for coordination, binding concurrently to the two Ag^I centers which participate in the argentophilic interaction. As a result of all the above, the two crystallographically independent metal centers of this compound possess a distorted trigonal bipyramidal (τ = 0.68[81]) coordination geometry, respectively.

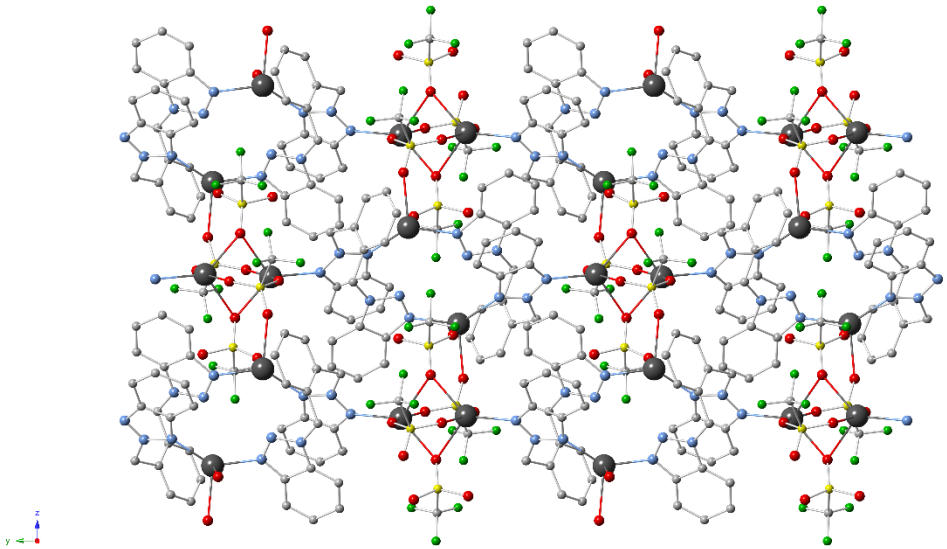

Figure 5. Part of the two-dimensional framework along the *b0c* plane in compound **8**. H atoms are omitted for clarity. Color code Ag (anthracite), C (light grey), N (light blue), O (red), F (green), S (yellow).

Table 1. Structural summary of compounds **1-13**.

Entry	Compound	Ligand	Coordination Environment of M (Ag^{I})	Solvent	Metal salt	Dimensionality
1	**1**	L^{1}		MeCN	$AgCF_3CO_2$	2D
2	**2**	L^{1T}		Me_2CO	$AgCF_3SO_3$	2D
3	**3**	L^{2T}		Me_2CO	$AgClO_4$	1D
4	**4**	L^{2T}	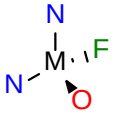	Me_2CO	$AgBF_4$	1D
5	**5**	L^{3T}		Me_2CO	$AgClO_4$	0D
6	**6**	L^{3}	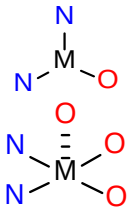	MeCN	$AgNO_3$	1D

7	**7**	L^{3T}	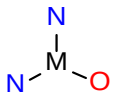	Me_2CO	$AgCF_3CO_2$	0D
8	**8**	L^{3T}	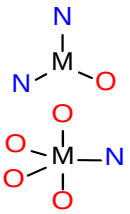	Me_2CO	$AgCF_3SO_3$	2D
9	**9**	L^{3T}	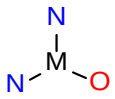	Me_2CO	$AgCF_3CF_2CO_2$	0D

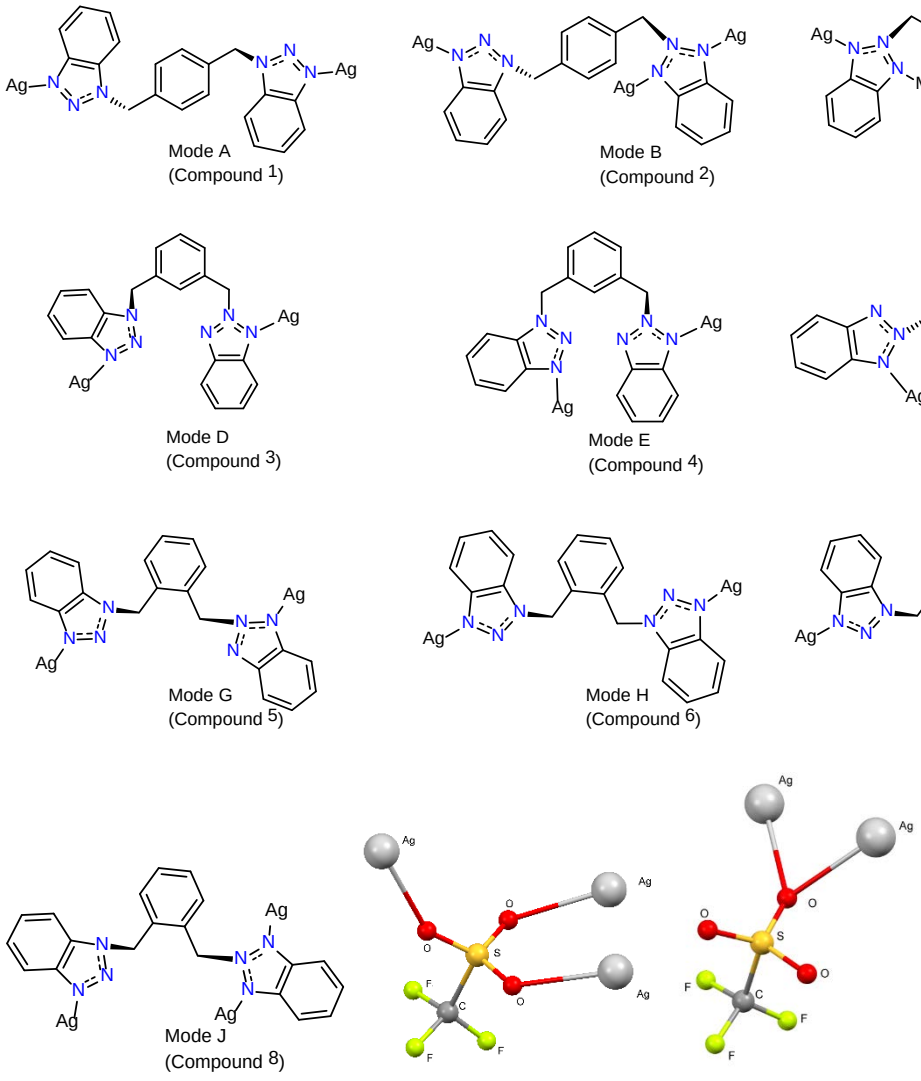

Scheme 2. (Modes A-J) The coordination modes for all ligands that appear in compounds **1**-**9**. (bottom middle and right) The coordination modes of the triflate anions in compound **8**.[82]

Characterization of compounds.

Thermogravimetric Analysis. TGA measurements were conducted for all compounds to examine their thermal stability. The results illustrate this behavior in the region of 50-1000°C. These experiments revealed similar outcomes, as in all cases the main (polymeric or dimeric) core retains its stability up to the region of ~220-300°C, where gradual decomposition begins to take place. Complex **1** shows a gradual mass loss in the 50-250°C range which is due to the removal of trifluoroacetate entities (calcd.: 20.45%, theor.: 20.18%). Almost immediately, the core is subjected to further gradual decomposition towards the final oxide (calcd.: 58.77%, theor.: 59.30%). In the case of complex **2**, the first mass loss (9.59%) occurs from 50 to 114°C and corresponds to the loss of the acetone lattice molecule in good agreement (theoretical value: 8.87%). The remaining core is stable until 291°C, where it collapses towards gradual decomposition. In compound **3**, the main core retains its stability until 297°C where it is decomposed to Ag_2O. The calculated (79.24%) and theoretical (78.96%) values are also in very good agreement. Compound **4** remains relatively stable until the region of 285°C (as the Et_2O molecule is lost before the TGA measurement begins) and the first mass loss corresponds to the collapse of the entire framework until decomposition (calcd.:= 82.94%,theor.: 81.14%). Complex **5** shows very similar thermal stability, retaining its main core up to 285°C before eventual collapse. In compound **6**, an initial mass loss of 11.60% occurs at approximately 273°C and finishes at 286°C, attributed to the loss of the nitrate anion (theor.: 12.15%). Decomposition of the remaining framework takes place almost immediately (calcd.: 65.65%, theor.: 65.33%). The structure of **7** remains relatively stable up to the region of 215°C, where a large mass loss occurs (81.73%), attributed to the collapse of the framework with reasonable agreement (theor: 79.48%). In complex **8**, there is initially a removal of the triflate anions (28.11% mass loss) from the framework which begins at 275°C and concludes at 310°C. Shortly after this point, the remaining structure collapses to eventual decomposition to silver

oxide (calcd.: 54.58%, theor.:55.59%). Finally, in compound **9** the first mass loss occurs until approximately 218°C and corresponds to the loss of the acetone lattice solvent molecule (calcd: 4.54%, theor: 5.96%). The second mass loss begins almost immediately (at the region of 220°C) and is owed to the collapse of the remaining compound up to decomposition (82.16% mass loss) with satisfactory agreement to the theoretical value (84.26%). The respective TGA graphs are presented in the Supporting Information (Figures S13-S21).

ESI-MS studies. Electrospray ionization mass spectrometry (ESI-MS) in methanolic solution was also performed for compounds **1**-**9**, to further verify their behavior. The resulting spectra are very similar for all complexes, with two peaks at 447.05 and 789.20 m/z which correspond to the relevant $[AgL]^+$ and $[AgL_2]^+$ fragments. These are the main peaks at all compounds with the exception of complex **6**; in this case, the main peaks correspond to ligand-based fragments and the aforementioned Ag-containing peaks are found in very low intensity, indicating that the polymer may not be so stable in solution. Several of the remaining compounds present additional peaks and the most common fragment is $[Ag_2L_2X]^+$, where X is the relevant anion in each case. Other peaks that are present in some compounds correspond perfectly to the $[AgL_3]^+$, $[Ag_2L_3X]^+$, $[Ag_3L_2X_2]^+$ and $[AgL_3X_2]^+$ fragments. All spectra are presented in Figures S22-S30 along with a detailed analysis of the fragments.

Isomerism effect and NMR studies. The tautomerism of heterocycles[83,84] is a very common phenomenon that has been extensively studied for several decades. Related reports[85–89] focusing specifically on benzotriazole and its derivatives began surfacing especially after the 1980s, including studies on relevant metal complexes[90–94]. Multiple efforts have documented that several types of substituted benzotriazole derivatives exist in solution as an equilibrium mixture of the corresponding 1- and 2-isomers[95–98]. Some of these cases include *N*-arylmethyl-[99], *N*-(aminomethyl)-[100,101], *N*-(alkoxyalkyl)-[102] and *N*-(alkylthioalkyl)- or *N*-(arylthioalkyl)-

benzotriazoles[103]. It has been shown[83,86,95] that the main parameters that affect the position of this equilibrium are i) solvent polarity, as a more polar solvent shifts the equilibrium towards the more polar 1-isomer, ii) temperature, as benzotriazole has been found to be stable as the 2-isomer in gas phase, and iii) the nature of the substituent, as the ratio of the 2-isomer increases in equilibrium when the bulkiness of the substituent is also increased. Interestingly, a search in the literature reveals no similar investigations for bis-benzotriazole substituted compounds. The present report contains several compounds with both isomer forms in three different bis-benzotriazole ligands, while the presence of Ag^{I} allows for possible NMR studies. We therefore felt this was an excellent opportunity to shed more light into this isomerism effect. The sole reported Ag^{I} compound with these ligands is a dimeric $[Ag_2(L^2)_3](NO_3)_2\cdot(MeCN)\cdot$compound as described by O'Keefe and Steel[104], in which only the 1,1-isomer form of L^2 is present in the crystal structure; unfortunately, no NMR studies were performed for the compound in that report.

We first established purity during the synthesis by obtaining crystals of the 1,1-isomer form for ligands L^1-L^3. Crystals of compounds **1**-**9** were then characterized with ^{1}HNMR in deuterated DMSO, as none of the complexes was soluble in $CDCl_3$. The obtained ppm shifts reveal interesting results: In general, the 1,1-isomer form exists almost solely (>99:1 ratio) in solution for compounds **1** and **6** results that is consistent with that determined in the crystal structure. Surprisingly, the corresponding 1,1-isomers were also obtained for compounds **2**-**4**, despite the exclusive presence of the 1,2-isomers in their crystal structures. On the other hand, both 1,1- and 1,2- isomers are present in the solution form for complexes **5**, **7**, **8** and **9** with various ratios (1:1, 1:1, 2:1 and 1:1 respectively). These results demonstrate that the 1,1- form is generally dominant in solution even in cases where the crystal structure does not contain this tautomer; however, the equilibrium may still move towards the 1,2-form in some cases. Having in mind that all NMR studies were performed under the same solvent and temperature

conditions, it can be proposed that the main reason for the presence of the 1,2-isomer is the nature of the substitution. This hypothesis is consistent with our findings for compounds **5**, **7**-**9** where the used substituent is increasing its bulky effect and the benzotriazole units are found in the *ortho*-position. From the crystal structure of these compounds it is evident that the *ortho*-substitution accounts for larger steric effects compared to the *para*- and *meta*-substituted structures. Additional intermolecular π···π and argentophilic interactions are also present in these complexes, possibly hindering the equilibrium shift to the 1,1-form even further. ^{15}N HMBC studies (Figures S40-S41) were also performed for selected compounds **4** and **6**. Both spectra show only a single resonance, originating from the -CH_2 linker, showing a 2JNH correlation to the pyrrole-like nitrogen of the triazole. The respective ^{15}N chemical shifts (referenced to CH_3NO_2) at -155.99 (for **4**) and -154.37 (for **6**) ppm are also consistent with a pyrrole-like nitrogen, suggesting the existence of 1,1-isomer in both compounds.

On the other hand, less clear conclusions may be drawn in regards to the parameters which promote the presence of the 1,2-isomer in the solid state. Synthetic conditions such as the temperature, metal:ligand ratio or crystallization method do not seem to have any noticeable effect. However, a correlation with the solvent choice and polarity during the initial synthesis may be proposed, as all 1,1-based compounds were afforded in acetonitrile (μ = 3.92 D), while the use of the slightly less polar acetone (μ = 2.88 D) resulted only in 1,2-based compounds. Interestingly, this pattern is additionally supported by two more compounds synthesized during our experiments, which are not presented in detail due to very weak crystallographic data. Both of these compounds, formulated as [Ag(L^2)($CF_3CF_2CO_2$)] and [Ag_2(L^2)$_3$](ClO_4)$_2$ (Figures S2-S3), were synthesized in acetonitrile and contain only the 1,1-isomer of the ligand. A comparison between the latter complex and compound [Ag(L^{2T})(ClO_4)(Me_2CO)](**3**) show that the choice of solvent could indeed play an important role. Moreover, the [Ag_2(L^2)$_3$](NO_3)$_2$(MeCN)·compound[104] was recrystallized in acetonitrile. However, this

phenomenon is only consistent for Ag^{I} complexes, as several Cu^{II} and Co^{II} compounds reported by us in previous studies did not exhibit similar behavior. As such, more studies are required to fully comprehend this effect.

Catalytic studies

A^3 coupling reaction. To initiate our investigations for the catalytic potential of **1-9** we first employed them in the multicomponent A^3 coupling of benzaldehyde, pyrrolidine and phenylacetylene, performing an extensive screening of all related parameters as seen in Table 2. All compounds proved to be ineffective in solvents such as water, DMF and DMSO (Table 2, entries 7 – 9, 23 – 25), however they provided low yields in the homogeneous catalysis of the reaction when other common organic solvents were used such as Toluene, THF, CH_3CN, CH_2Cl_2 and $CHCl_3$ (Table 2, entries 6, 10 – 13, 22, 26 – 29). In general, the highest yields were achieved through the use of polar alcoholic solvents and especially with the environmentally friendly solvent[105] 2-propanol (iPrOH) when the reaction mixture was heated to 90^{o}C for 12 hours. All compounds were found to catalyze the reaction under these conditions (Table 2, entries 4-5, 14-15, 19-21, 32-36); amongst these, the 1D CP **4** afforded the corresponding product at excellent yields of 94%, with very low loadings of 0.5 mol% used (TOF = 188 and TON = 15.7 hr^{-1}, calculated with the ratio of product mol/catalyst mol). To further evaluate the efficiency of **4**, we compared the performances of all reported Ag^{I} sources which have been tested in the model reaction to the best of our knowledge, including simple salts, coordination polymers and coordination compounds (Table S8). To our delight, **4** emerges as a highly advantageous catalyst in many aspects, due to the resulting excellent yield and TOF number which outperforms many of the reported Ag sources (Table S8, entries 1-8). On the other hand, the stirring times in the case of our catalyst appear to be longer than those usually reported[41,42,56,57,60,106]. Despite this, the conditions of our proposed reaction system appear to be less harsh or tedious (e.g. no N_2 atmosphere or environmentally unfriendly solvent

is needed). Various Ag^{I} salts were also tested under the same conditions (Table S8, entries 10-15) showing slightly inferior performance, further indicating the superiority of **4**.

Table 2. Optimization of the conditions for the synthesis of propargylamines.

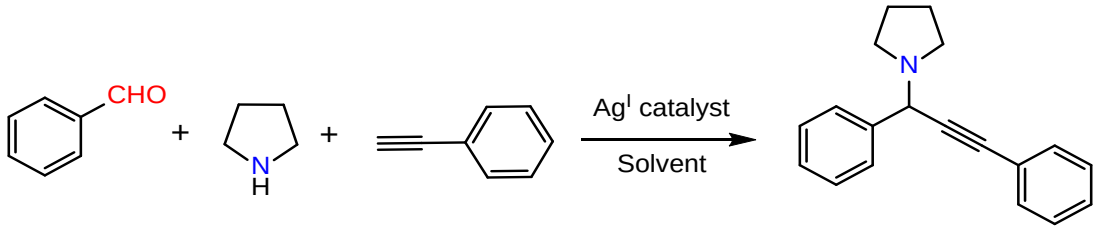

Entry	Catalyst (mol%)[a]	Solvent	Yield (%)[b]	TON	TOF (hr^{-1})
1	**1** (2)	MeOH	trace	-	-
2	**1** (2)	EtOH	18	9	0.8
3	**1** (2)	iPrOH	28	14	1.2
4	**1** (2)	iPrOH[c]	85	43	3.6
5	**1** (0.5)	iPrOH[c]	83	166	13.8
6	**1** (2)	Toluene	14	7	0.6
7	**1** (2)	H_2O	NR[d]	-	-
8	**1** (2)	DMF	NR[d]	-	-
9	**1** (2)	DMSO	NR[d]	-	-
10	**1** (2)	THF	10	5	0.4
11	**1** (2)	MeCN	13	7	0.6
12	**1** (2)	CH_2Cl_2	11	6	0.5
13	**1** (2)	$CHCl_3$	14	7	0.6
14	**2** (0.5)	iPrOH[c]	81	162	13.5
15	**3** (0.5)	iPrOH[c]	88	176	14.7

16	**4** (2)	MeOH	<10	-	-
17	**4** (2)	EtOH	16	8	0.7
18	**4** (2)	iPrOH	29	15	1.3
19	**4** (2)	iPrOH[c]	95	48	4
20	**4** (1)	iPrOH[c]	94	94	7.8
21	**4** (0.5)	iPrOH[c]	94	188	15.7
22	**4** (2)	Toluene	18	9	0.8
23	**4** (2)	H_2O	NR[d]	-	-
24	**4** (2)	DMF	NR[d]	-	-
25	**4** (2)	DMSO	NR[d]	-	-
26	**4** (2)	THF	<10	-	-
27	**4** (2)	MeCN	11	6	0.5
28	**4** (2)	CH_2Cl_2	15	8	0.7
29	**4** (2)	$CHCl_3$	16	8	0.7
30	**4** (0.5)[e]	iPrOH[c]	63	126	21
31	**4** (0.5)[f]	iPrOH[c]	94	188	7.8
32	**5** (0.5)	iPrOH[c]	70	140	11.7
33	**6** (0.5)	iPrOH[c]	81	162	13.5
34	**7** (0.5)	iPrOH[c]	66	132	11
35	**8** (0.5)	iPrOH[c]	71	142	11.8
36	**9** (0.5)	iPrOH[c]	74	148	12.3
37	No catalyst	iPrOH[c]	NR[d]	-	-

[a] Reaction conditions: benzaldehyde (25 μL, 0.25 mmol), pyrrolidine (22 μL, 0.275 mmol), phenylacetylene (43 μL, 0.4 mmol), catalyst (mol% based on aldehyde amount), solvent (3 ml), 12 hr stirring, air. [b] Isolated yields based on aldehyde. [c] T = 90°C. [d] No reaction. [e] under 6 hrs stirring. [f] under 24 hrs stirring.

Having determined the optimal efficiency, we further investigated the substrate scope of our system using **4** as the catalyst. Various aldehydes, amines and alkynes were coupled under the proposed conditions and the results are shown in Scheme 3. We began by exploring the effect of the aldehyde, retaining pyrrolidine and phenylacetylene as the model substrates.

In all cases the corresponding A^3 products **13a-13i** were formed in good to high isolated yields, however the substituted aromatic aldehydes show lower reactivity, allowing for more moderate (64-89%) yields and sometimes requiring higher catalyst loading. In contrast, saturated aliphatic aldehydes display excellent reactivity and provide very high (98-99%) yields, irrespective of whether the tested substrate is cyclic or linear. Having this in mind, we proceeded on the amine screening by employing cyclohylcarbaldehyde and phenylacetylene as the remaining two model substrates. These tests showed that the proposed reaction system is ideal for secondary amines, as the resulting products are afforded in excellent yields of 93 to 99% (**13i-13o**). There are seemingly no restrictions in the choice of secondary amine, as similar results were obtained for cyclic or linear aliphatic and aromatic substrates. However, this behavior seems to be limited as no reaction was observed when primary amines were used (entries **13p** and **13q**). Finally in regards to the alkyne selection, the use of either phenylacetylene or 1-hexyne resulted to the corresponding propargylamines in excellent yields, **13i** and **13r** in 99% and 98%, respectively.

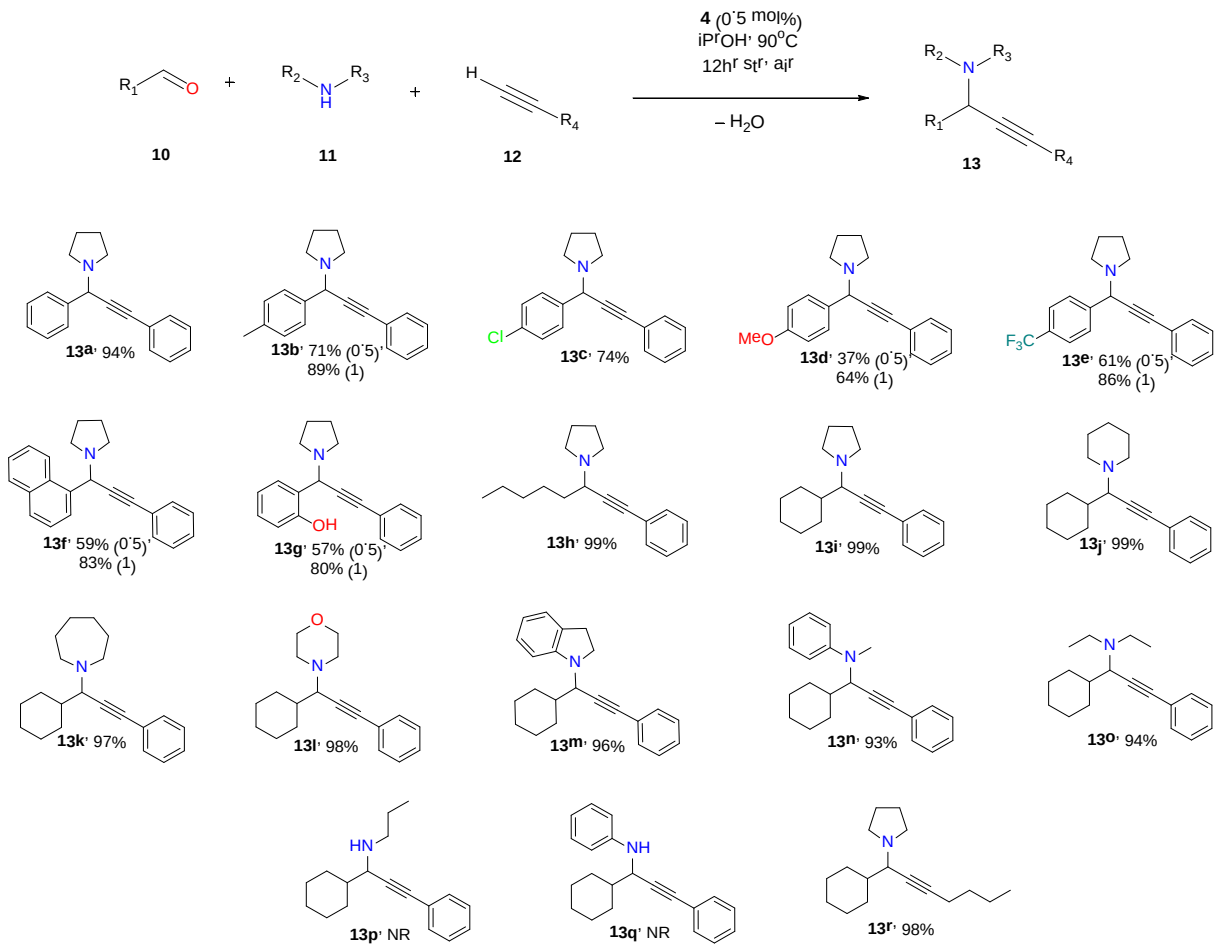

Scheme 3. Catalytic activity of **4** in the A^3 coupling between various aldehydes, amines and alkynes towards propargylamine synthesis.

A possible mechanism for this multicomponent coupling on the basis of many reported proposals is presented in Scheme 4. It involves the activation of the alkyne by the silver catalyst to form a metal-acetylide π-complex intermediate. Concurrently, the addition of aldehyde and amine results to the generation of an iminium ion *in situ*; the hydroxyl anions produced during the formation of this species might also assist in the abstraction of the acetylenic proton. In the last step of the catalytic cycle the Ag^I-acetylide is added to this iminium ion to produce the corresponding propargylamine derivative and water, as the catalyst is regenerated. We envision that the formation of the metal-acetylide intermediate could also be influenced by the coordination and geometric characteristics of our catalytic precursors; both compounds **3** and

4, which resulted in the highest yields in our experiments, possess a trigonal $\{N_2X\}$ environment (CHN and TGA studies show that all other coordinating solvents contained are removed from the frameworks at slightly above room temperature) that provides adequate space and possibly promotes the coordination of the alkyne. The helix-like chain in **4**, owed to the flexibility of the $-CH_2$ linkers which leads to almost parallel conformation of the benzotriazole planes, accounts for further space between the Ag^I centers, with the Ag-Ag distance measured at 10.3143(9) Å, the largest between these two complexes. It is also worth noting that the dimeric core compounds (**5**, **7** and **9**) of the study resulted in lower yields in all cases. We can therefore suggest that the use of polymeric precursors leads to the formation of the most catalytically active species and is essential for optimal efficiency in the reaction.

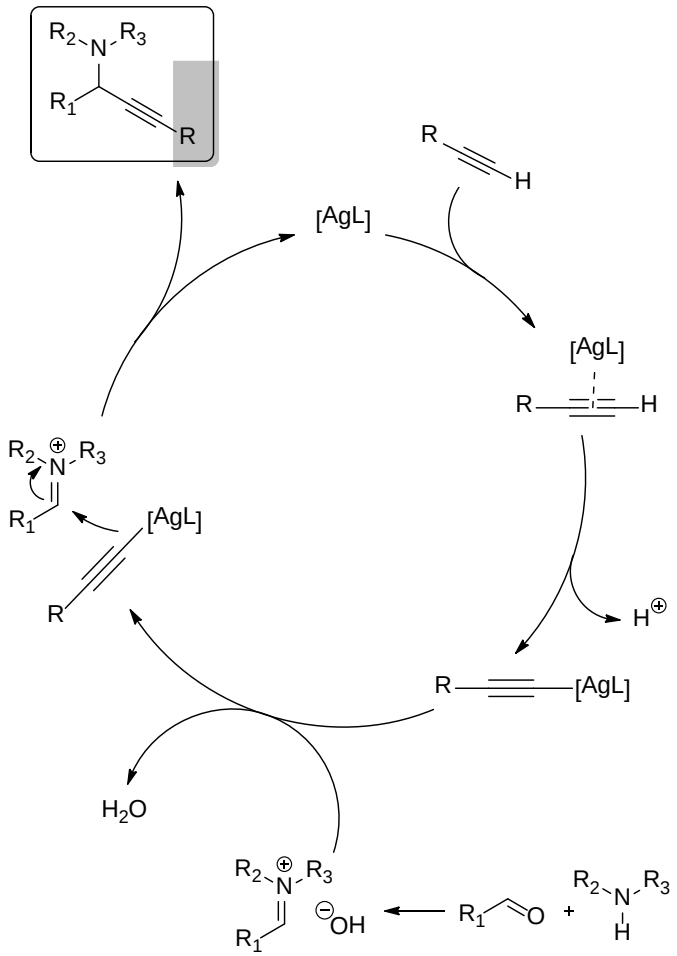

Scheme 4. A plausible mechanism of the A^3 coupling catalyzed by **4**.

Hydration of alkynes

The selective hydration of alkynes is an important transformation in organic chemistry. When Markovnikov's rule is followed, the reaction leads to the formation of ketones, which are very important due to their abundance in natural products and their extensive use as building blocks in organic synthesis. For our experiments, we used **4** towards the hydration of phenylacetylene in various solvent/water systems in a 10/1 ratio. The outcomes of these screenings are shown in Table 3. To our delight, this procedure selectively affords the resulting acetophenone in an excellent yield 93%, when MeOH/H_2O is used as the solvent system, under 90°C for 24 hours and 3 mol% catalyst loading, with TON = 31.0 and TOF = 1.32 hr^{-1} (Table 3, entry 3). The presence of alcoholic media and temperature appears to be essential for the system (Table 3, entries 3, 5 and 8), as no product was afforded when the reaction took place under room temperature or other solvents such as CH_3CN and EtOAc (Table 3, entries 6 and 7). The other catalytic compounds **1**-**3** and **5**-**9** of this study were also examined in the reaction (Table 3, entries 9-16), providing lower yields. Compound **3** shows the best catalytic activity compared to the others, catalyzing the reaction in an excellent 86% yield. This result further supports our above suggestion that the coordination characteristics of **3** and **4** promote the formation of the silver-acetylide intermediate. Interestingly, none of the dimeric compounds of the study afforded the corresponding ketone, as the only remaining compounds that promoted the reaction were the 2D CPs **1**, **2** and **8** with moderate to good yields (Table 3, entries 9, 10 and 15 respectively).

The hydration of other terminal alkynes using **4** was also tested successfully (Scheme 5) under the optimal conditions. The presence of a methoxy- substituent in the initial alkyne does not appear to affect the reaction as the corresponding 4-methoxyacetophenone (**5b**) was produced in 94% yield. Furthermore, to evaluate the catalytic ability of this system with

aliphatic alkynes we employed the linear 1-hexyne under the same conditions, forming the corresponding ketone in good conversions (**15c**, in 66% yield).

We envision that the mechanism proceeds in a commonly proposed pathway (Scheme 6) in which the silver-acetylide species (**A**) is formed in the first step, possibly promoted by the coordination environment of the catalyst as well as the use of the protic solvent methanol. It is highly likely, by analogy with Belanzoni and Zuccaccia's mechanistic studies on gold catalyzed hydration reactions,[107] that our ligand is facilitating the reaction through electrostatic interaction between water and the ligand(s) *via* hydrogen bonding to one of the Brønsted-basic nitrogens. This chelation directs H_2O during the addition reaction to generate the enol intermediate (**B**) and the ligand can subsequently assist with the proton transfer from the newly formed oxonium. **B** then undergoes keto–enol tautomerism to produce (**C**) which subsequently undergoes proto-demetalation to generate the resulting ketone (**D**). Importantly, the best results are of great eco-friendly impact, with low catalyst loading and acid-free conditions, and requiring environmentally-benign methanol as solvent.

Table 3. Optimization experiments for the hydration of phenylacetylene to acetophenone.

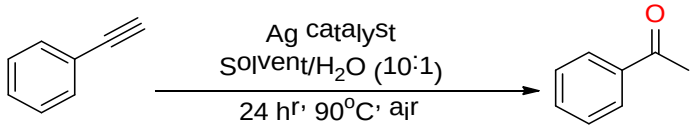

Entry	Catalyst (mol%)	Solvent	Yield(%)[a, b]	TON	TOF (hr^{-1})
1	**4** (0.5)	MeOH	66	22.0	0.92
2	**4** (1)	MeOH	74	24.7	1.03
3	**4** (3)	MeOH	93	31.0	1.32
4	**4** (3)	MeOH	NR[c,d]	-	-
5	**4** (3)	EtOH	77	25.7	1.07
6	**4** (3)	MeCN	NR[c]	-	-
7	**4** (3)	EtOAc	NR[c]	-	-
8	**4** (3)	iPrOH	65	21.7	0.90

9	**1** (3)	MeOH	44	14.7	0.61
10	**2** (3)	MeOH	60	20.0	0.83
11	**3** (3)	MeOH	86	28.7	1.20
12	**5** (3)	MeOH	NR[c]	-	-
13	**6** (3)	MeOH	NR[c]	-	-
14	**7** (3)	MeOH	NR[c]	-	-
15	**8** (3)	MeOH	66	22.0	0.92
16	**9** (3)	MeOH	NR[c]	-	-

[a] Isolated yield based on alkyne. [b] Reaction conditions: phenylacetylene (121 µL, 1 mmol), catalyst, solvent (1.5 ml), H_2O (150 µl), 90°C, 24 hr stirring, air. [c] No reaction. [d] At room temperature.

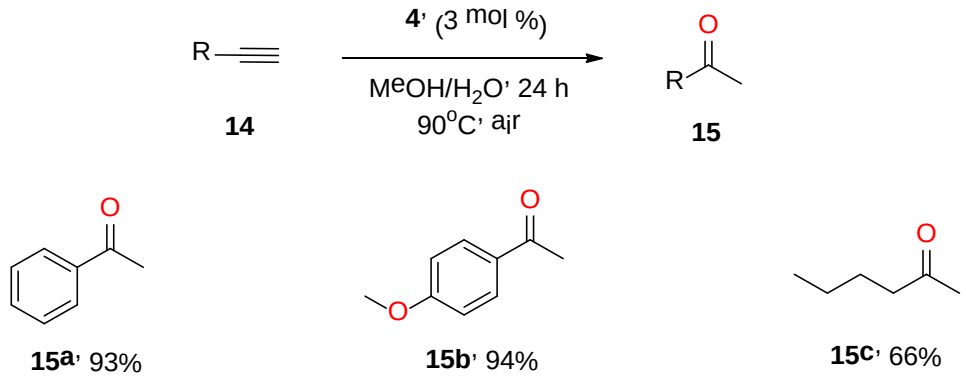

Scheme 5. Catalytic activity of **4** in the hydration of alkynes to ketones.

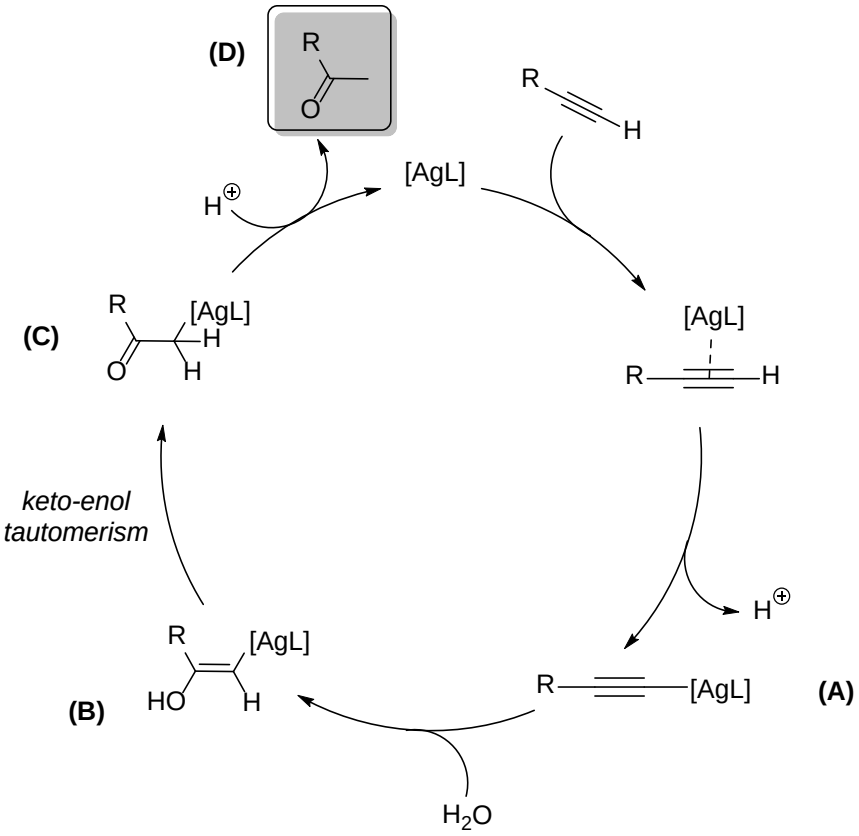

Scheme 6. A plausible mechanism of the hydration of alkynes catalyzed by **4**.

CONCLUSION

In this study, we have attempted to combine the rich chemistry and coordination capabilities of Ag^{I} ions with a series of semi-rigid benzotriazole-based ligands L^{1}-L^{3}. The resulting compounds **1**-**9** exhibit a large structural diversity that includes a range of 0D dimers and 1D / 2D coordination polymers with interesting topological features and architectures as well as peculiar isomerism effects observed. An important factor for the variety in these coordination networks is owed to the flexibility of the ligands, which accounts for multiple coordination modes. The complexes have also been investigated for their potential catalytic applications. Due to its structural nature and coordination characteristics, compound **4** serves as homogeneous catalyst in A^{3} coupling and alkyne hydration reactions, providing the respective propargylamines and ketones in generally excellent yields (up to 99 and 93% in each case) that are comparable or superior to the ones of other reported Ag^{I}-based catalysts. Both proposed reaction schemes include easy synthetic conditions and avoid the use of inert atmosphere or environmentally harsh solvents. Furthermore, the superior alkynophilicity of Ag^{I} compared to Cu^{II} makes **4** a favorable option against the relevant Cu^{II}-based coordination polymers with reported[49] catalytic performance, as high yields are achieved with much lower catalyst loadings (0.5 mol% compared to 2 mol%). Encouraged by these results, future work will focus on using this structural information to expand our scope to additional N-containing flexible ligands with Ag^{I} sources and tune their coordination environment to optimize their application potential.

ACKNOWLEDGEMENTS

We thank the EPSRC UK National Crystallography Service at the University of Southampton for the collection of the crystallographic data for for **6**, **7** and **9**.[68]

ASSOCIATED CONTENT

Supporting Information

The Supporting Information is available free of charge on the ACS Publications website at DOI: 10.1021/acs.cgd.7b00200.

Crystallographic data, additional figures of crystal structures, characterization data of the Ag compounds (IR, TGA, ESI-MS, , 1H-NMR, ^{15}N HMBC NMR spectrum of **6**) evaluation of catalytic conditions and performance, characterization data of products (^{1}H, ^{13}C NMR and HRMS spectra)

Accession Codes

CCDC 1851153-1851162 contain the supplementary crystallographic data for this paper. These data can be obtained free of charge via www.ccdc.cam.ac.uk/data_request/cif, or by emailing data_request@ccdc.cam.ac.uk, or by contacting The Cambridge Crystallographic Data Centre, 12 Union Road, Cambridge CB2 1EZ, UK; fax: +44 1223 336033.

REFERENCES

(1) Desiraju, G. R. Crystal Engineering: From Molecule to Crystal. *J. Am. Chem. Soc.* **2013**, *135*, 9952–9967.

(2) Fujita, M.; Washizu, S.; Ogura, K.; Kwon, Y. J. Preparation, Clathration Ability, and Catalysis of a Two-Dimensional Square Network Material Composed of Cadmium(II) and 4, 4′-Bipyridine. *J. Am. Chem. Soc.* **1994**, *116*, 1151–1152.

(3) Tannenbaum, R. Three-Dimensional Coordination Polymers of Ruthenium(2+) with 1,4-Diisocyanobenzene Ligands and Their Catalytic Activity. *Chem. Mater.* **1994**, *6*, 550–555.

(4) Leong, W. L.; Vittal, J. J. One-Dimensional Coordination Polymers: Complexity and Diversity in Structures, Properties, and Applications. *Chem. Rev.* **2011**, *111*, 688–764.

(5) Loukopoulos, E.; Kostakis, G. E. Recent Advances of One-Dimensional Coordination Polymers as Catalysts. *J. Coord. Chem.* **2018**, *71*, 1–40.

(6) Kirillov, A. M.; Karabach, Y. Y.; Kirillova, M. V; Haukka, M.; Pombeiro, A. J. L. Topologically Unique 2D Heterometallic Cu II/Mg Coordination Polymer: Synthesis, Structural Features, and Catalytic Use in Alkane Hydrocarboxylation. *Cryst. Growth Des.* **2012**, *12*, 1069–1074.

(7) Yu, F.; Xiong, X.; Huang, K.; Zhou, Y.; Li, B. 2D Co-Based Coordination Polymer with a Histidine Derivative as an Efficient Heterogeneous Catalyst for the Oxidation of Cyclohexene. *CrystEngComm* **2017**, *19*, 2126–2132.

(8) Gupta, M.; De, D.; Pal, S.; Pal, T. K.; Tomar, K. A Porous Two-Dimensional Zn(Ii)-Coordination Polymer Exhibiting SC–SC Transmetalation with Cu(Ii): Efficient Heterogeneous Catalysis for the Henry Reaction and Detection of Nitro Explosives. *Dalton. Trans.* **2017**, *46*, 7619–7627.

(9) da Silva, G. B.; Menezes, P. H.; Malvestiti, I.; Falcão, E. H. L.; Alves, S.; Chojnacki, J.; da Silva, F. F. Copper-Based 2D-Coordination Polymer as Catalyst for Allylation of Aldehydes. *J. Mol. Struct.* **2018**, *1155*, 530–535.

(10) Fernandes, T. A.; Santos, C. I. M.; André, V.; Kłak, J.; Kirillova, M. V.; Kirillov, A. M. Copper(II) Coordination Polymers Self-Assembled from Aminoalcohols and Pyromellitic Acid: Highly Active Precatalysts for the Mild Water-Promoted Oxidation of Alkanes. *Inorg. Chem.* **2016**, *55*, 125–135.

(11) Corma, A.; García, H.; Llabrés i Xamena, F. X. Engineering Metal Organic Frameworks for Heterogeneous Catalysis. *Chem. Rev.* **2010**, *110*, 4606–4655.

(12) Zhu, L.; Liu, X. Q.; Jiang, H. L.; Sun, L. B. Metal-Organic Frameworks for Heterogeneous Basic Catalysis. *Chem. Rev.* **2017**, *117*, 8129–8176.

(13) Huang, Y.-B.; Liang, J.; Wang, X.-S.; Cao, R. Multifunctional Metal–organic Framework Catalysts: Synergistic Catalysis and Tandem Reactions. *Chem. Soc. Rev.* **2017**, *46*, 126–157.

(14) Cotton, F. A.; Wilkinson, G. *Advanced Inorganic Chemistry*, 5th ed.; Wiley, Ed.; Wiley, 1988.

(15) Du, J.-L.; Hu, T.-L.; Zhang, S.-M.; Zeng, Y.-F.; Bu, X.-H. Tuning Silver(I) Coordination Architectures by Ligands Design: From Dinuclear, Trinuclear, to 1D and 3D

Frameworks. *CrystEngComm* **2008**, *10*, 1866.

(16) Chi, Y. N.; Huang, K. L.; Cui, F. Y.; Xu, Y. Q.; Hu, C. W. Structural Diversity of Silver(I) 4,6-Dipyridyl-2-Aminopyrimidine Complexes: Effect of Counteranions and Ligand Isomerism. *Inorg. Chem.* **2006**, *45*, 10605–10612.

(17) Tatikonda, R.; Bulatov, E.; Kalenius, E.; Haukka, M. Construction of Coordination Polymers from Semirigid Ditopic 2,2′-Biimidazole Derivatives: Synthesis, Crystal Structures, and Characterization. *Cryst. Growth Des.* **2017**, *17*, 5918–5926.

(18) Bassanetti, I.; Atzeri, C.; Tinonin, D. A.; Marchiò, L. Silver(I) and Thioether-Bis(Pyrazolyl)Methane Ligands: The Correlation between Ligand Functionalization and Coordination Polymer Architecture. *Cryst. Growth Des.* **2016**, *16*, 3543–3552.

(19) Davarci, D.; Gür, R.; Beşli, S.; Şenkuytu, E.; Zorlu, Y. Silver(I) Coordination Polymers Assembled from Flexible Cyclotriphosphazene Ligand: Structures, Topologies and Investigation of the Counteranion Effects. *Acta Crystallogr. Sect. B Struct. Sci. Cryst. Eng. Mater.* **2016**, *72*, 344–356.

(20) Yeh, C. W.; Tsou, C. H.; Tsai, H. A.; Lee, H. T.; Yao, W. H.; Suen, M. C. Structural Diversity in the Self-Assembly of Silver(I) Complexes Containing 2,6-Dimethyl-3,5-Dicyano-4-(4-Quinolinyl)-1,4-Dihydropyridine. *Inorganica Chim. Acta* **2015**, *427*, 1–12.

(21) Lamming, G.; Kolokotroni, J.; Harrison, T.; Penfold, T. J.; Clegg, W.; Waddell, P. G.; Probert, M. R.; Houlton, A. Structural Diversity and Argentophilic Interactions in One-Dimensional Silver-Based Coordination Polymers. *Cryst. Growth Des.* **2017**, *17*, 5753–5763.

(22) Janiak, C.; Scharmann, T. G.; Albrecht, P.; Marlow, F.; Macdonald, R. [Hydrotris(1,2,4-Triazolyl)Borato]Silver(I): Structure and Optical Properties of a Coordination Polymer Constructed from a Modified Poly(Pyrazolyl)Borate Ligand. *J. Am. Chem. Soc.* **1996**,

118, 6307–6308.

(23) Wu, H.-P.; Janiak, C.; Rheinwald, G.; Lang, H. 5,5′-Dicyano-2,2′-Bipyridine Silver Complexes: Discrete Units or Co-Ordination Polymers through a Chelating and/or Bridging Metal–ligand Interaction. *J. Chem. Soc. Dalt. Trans.* **1999**, 183–190.

(24) Munakata, M.; Wu, L. P. Solid-State Supramolecular Metal Complexes Containing Copper(I) and Silver(I). *Adv. Inorg. Chem.* **1999**, *46*, 173–303.

(25) Khlobystov, A. N.; Blake, A. J.; Champness, N. R.; Lemenovskii, D. A.; Majouga, A. G.; Zyk, N. V.; Schröder, M. Supramolecular Design of One-Dimensional Coordination Polymers Based on Silver(I) Complexes of Aromatic Nitrogen-Donor Ligands. *Coord. Chem. Rev.* **2001**, *222*, 155–192.

(26) Wang, Y.-L.; Liu, Q.-Y.; Xu, L. Two Novel Luminescent Silver(I) Coordination Polymers Containing Octanuclear Silver Cluster Units or Ligand Unsupported Ag···Ag Interactions Constructed from 5-Sulfoisophthalic Acid (H3SIP) and Organic Amine. *CrystEngComm* **2008**, *10*, 1667.

(27) Du, L. Y.; Shi, W. J.; Hou, L.; Wang, Y. Y.; Shi, Q. Z.; Zhu, Z. Solvent or Temperature Induced Diverse Coordination Polymers of Silver(I) Sulfate and Bipyrazole Systems: Syntheses, Crystal Structures, Luminescence, and Sorption Properties. *Inorg. Chem.* **2013**, *52*, 14018–14027.

(28) Roy, S.; Titi, H. M.; Tripuramallu, B. K.; Bhunia, N.; Verma, R.; Goldberg, I. Silver Coordination Polymers Based on Newly Designed Bis(Cyanobenzyl)Bipiperidine Ligand: Synthesis, Anion Exchange, Guest Inclusion, Electrochemical, and Photoluminescence Properties. *Cryst. Growth Des.* **2016**, *16*, 2814–2825.

(29) Min, K. S.; Suh, M. P. Silver(I)-Polynitrile Network Solids for Anion Exchange: Anion-Induced Transformation of Supramolecular Structure in the Crystalline State. *J. Am. Chem. Soc.* **2000**, *122*, 6834–6840.

(30) Li, C. P.; Zhou, H.; Mu, Y. H.; Guo, W.; Yan, Y.; Du, M. Structural Transformations Induced by Selective and Irreversible Anion Exchanges for a Layered Ag(I) Nitrite Coordination Polymer. *Cryst. Growth Des.* **2017**, *17*, 2024–2033.

(31) Azócar, M. I.; Gómez, G.; Levín, P.; Paez, M.; Muñoz, H.; Dinamarca, N. Review: Antibacterial Behavior of Carboxylate Silver(I) Complexes. *J. Coord. Chem.* **2014**, *67*, 3840–3853.

(32) Cardoso, J. M. S.; Galvão, A. M.; Guerreiro, S. I.; Leitão, J. H.; Suarez, A. C.; Carvalho, M. F. N. N. Antibacterial Activity of Silver Camphorimine Coordination Polymers. *Dalton. Trans.* **2016**, *45*, 7114–7123.

(33) Tăbăcaru, A.; Pettinari, C.; Marchetti, F.; Di Nicola, C.; Domasevitch, K. V.; Galli, S.; Masciocchi, N.; Scuri, S.; Grappasonni, I.; Cocchioni, M. Antibacterial Action of 4,4′-Bipyrazolyl-Based Silver(I) Coordination Polymers Embedded in PE Disks. *Inorg. Chem.* **2012**, *51*, 9775–9788.

(34) Jimenez, J.; Chakraborty, I.; Rojas-Andrade, M.; Mascharak, P. K. Silver Complexes of Ligands Derived from Adamantylamines: Water-Soluble Silver-Donating Compounds with Antibacterial Properties. *J. Inorg. Biochem.* **2017**, *168*, 13–17.

(35) Jimenez, J.; Chakraborty, I.; Del Cid, A. M.; Mascharak, P. K. Five- and Six-Coordinated Silver(I) Complexes Derived from 2,6-(Pyridyl)Iminodiadamantanes: Sustained Release of Bioactive Silver toward Bacterial Eradication. *Inorg. Chem.* **2017**, *56*, 4784–4787.

(36) Jaros, S. W.; Guedes Da Silva, M. F. C.; Król, J.; Conceição Oliveira, M.; Smoleński, P.; Pombeiro, A. J. L.; Kirillov, A. M. Bioactive Silver-Organic Networks Assembled from 1,3,5-Triaza-7-Phosphaadamantane and Flexible Cyclohexanecarboxylate Blocks. *Inorg. Chem.* **2016**, *55*, 1486–1496.

(37) Jaros, S. W.; Guedes Da Silva, M. F. C.; Florek, M.; Oliveira, M. C.; Smoleński, P.;

Pombeiro, A. J. L.; Kirillov, A. M. Aliphatic Dicarboxylate Directed Assembly of Silver(I) 1,3,5-Triaza-7-Phosphaadamantane Coordination Networks: Topological Versatility and Antimicrobial Activity. *Cryst. Growth Des.* **2014**, *14*, 5408–5417.

(38) Wu, X. Y.; Qi, H. X.; Ning, J. J.; Wang, J. F.; Ren, Z. G.; Lang, J. P. One Silver(I)/Tetraphosphine Coordination Polymer Showing Good Catalytic Performance in the Photodegradation of Nitroaromatics in Aqueous Solution. *Appl. Catal. B Environ.* **2015**, *168–169*, 98–104.

(39) Zhou, Z.; He, C.; Yang, L.; Wang, Y.; Liu, T.; Duan, C. Alkyne Activation by a Porous Silver Coordination Polymer for Heterogeneous Catalysis of Carbon Dioxide Cycloaddition. *ACS Catal.* **2017**, *7*, 2248–2256.

(40) Kulovi, S.; Dalbera, S.; Das, S.; Zangrando, E.; Puschmann, H.; Dalai, S. New Silver(I) Coordination Polymers with Hetero Donor Ligands: Synthesis, Structure, Luminescence Study and Photo-Catalytic Behavior. *ChemistrySelect* **2017**, *2*, 9029–9036.

(41) Sharma, K. N.; Sharma, A. K.; Joshi, H.; Singh, A. K. Polymeric Complex of 1-Phenylsulfanyl/Selenylmethyl-1 H -Benzotriazole with Ag(I): Pre-Catalystfor A 3 Coupling Affording Propargylamines on AGram/Lab Scale. *ChemistrySelect* **2016**, *1*, 3573–3579.

(42) Zhao, Y.; Zhou, X.; Okamura, T.-A.; Chen, M.; Lu, Y.; Sun, W.-Y.; Yu, J.-Q. Silver Supramolecule Catalyzed Multicomponent Reactions under Mild Conditions. *Dalton. Trans.* **2012**, *41*, 5889–5896.

(43) Chen, M.-M.; Li, H.-X.; Lang, J.-P. Two Coordination Polymers and Their Silver(I)-Doped Species: Synthesis, Characterization, and High Catalytic Activity for the Photodegradation of Various Organic Pollutants in Water. *Eur. J. Inorg. Chem.* **2016**, *2016*, 2508–2515.

(44) Ming, C. L.; Li, Y. H.; Li, G. Y.; Cui, G. H. Synthesis, Crystal Structures, Luminescence

and Catalytic Properties of Three Silver(I) Coordination Polymers with Bis(Imidazole) and Benzenedicarboxylic Acid Ligands. *Transit. Met. Chem.* **2014**, *39*, 477–485.

(45) Fang, G.; Bi, X. Silver-Catalysed Reactions of Alkynes: Recent Advances. *Chem. Soc. Rev.* **2015**, *44*, 8124–8173.

(46) Abbiati, G.; Rossi, E. Silver and Gold-Catalyzed Multicomponent Reactions. *Beilstein Journal of Organic Chemistry*. **2014**, 481–513.

(47) Loukopoulos, E.; Chilton, N. F.; Abdul-Sada, A.; Kostakis, G. E. Exploring the Coordination Capabilities of a Family of Flexible Benzotriazole-Based Ligands Using Cobalt(II) Sources. *Cryst. Growth Des.* **2017**, *17*, 2718–2729.

(48) Kallitsakis, M.; Loukopoulos, E.; Abdul-Sada, A.; Tizzard, G. J.; Coles, S. J.; Kostakis, G. E.; Lykakis, I. N. A Copper-Benzotriazole-Based Coordination Polymer Catalyzes the Efficient One-Pot Synthesis of (*N*′-Substituted)-Hydrazo-4-Aryl-1,4-Dihydropyridines from Azines. *Adv. Synth. Catal.* **2017**, *359*, 138–145.

(49) Loukopoulos, E.; Kallitsakis, M.; Tsoureas, N.; Abdul-Sada, A.; Chilton, N. F.; Lykakis, I. N.; Kostakis, G. E. Cu(II) Coordination Polymers as Vehicles in the A3 Coupling. *Inorg. Chem.* **2017**, *56*, 4898–4910.

(50) Andreou, D.; Kallitsakis, M.; Loukopoulos, E.; Gabriel, C.; Kostakis, G. E.; Lykakis, I. N. Copper-Promoted Regioselective Synthesis of Polysubstituted Pyrroles from Aldehydes, Amines and Nitroalkenes via 1,2-Phenyl/Alkyl Migration. *J. Org. Chem.* **2018**, *83*, 2104–2113.

(51) Arcadi, A.; Cacchi, S.; Cascia, L.; Fabrizi, G.; Marinelli, F. Preparation of 2 , 5-Disubstituted Oxazoles from N -Propargylamides. *Org. Lett.* **2001**, *16*, 2501–2504.

(52) Chauhan, D. P.; Varma, S. J.; Vijeta, A.; Banerjee, P.; Talukdar, P. A 1,3-Amino Group Migration Route to Form Acrylamidines. *Chem Commun* **2014**, *50*, 323–325.

(53) Yamamoto, Y.; Hayashi, H.; Saigoku, T.; Nishiyama, H. Domino Coupling Relay

Approach to Polycyclic Pyrrole-2-Carboxylates. *J. Am. Chem. Soc.* **2005**, *127*, 10804–10805.

(54) Peshkov, V. a.; Pereshivko, O. P.; Van der Eycken, E. V. A Walk around the A3-Coupling. *Chem. Soc. Rev.* **2012**, *41*, 3790.

(55) Halbes-Letinois, U.; Weibel, J.-M.; Pale, P. The Organic Chemistry of Silver Acetylides. *Chem. Soc. Rev.* **2007**, *36*, 759.

(56) Wei, C.; Li, Z.; Li, C.-J. The First Silver-Catalyzed Three-Component Coupling of Aldehyde, Alkyne, and Amine. *Org. Lett.* **2003**, *5*, 4473–4475.

(57) Prakash, O.; Joshi, H.; Kumar, U.; Sharma, A. K.; Singh, A. K. Acridine Based (S,N,S) Pincer Ligand: Designing Silver(i) Complexes for the Efficient Activation of A3 (Aldehyde, Alkyne and Amine) Coupling. *Dalton Trans.* **2015**, *44*, 1962–1968.

(58) Chen, J. J.; Gan, Z. L.; Huang, Q.; Yi, X. Y. Well-Defined Dinuclear Silver Phosphine Complexes Based on Nitrogen Donor Ligand and Their High Efficient Catalysis for A3-Coupling Reaction. *Inorganica Chim. Acta* **2017**, *466*, 93–99.

(59) Trivedi, M.; Singh, G.; Kumar, A.; Rath, N. P. Silver(I) Complexes as Efficient Source for Silver Oxide Nanoparticles with Catalytic Activity in A3 Coupling Reactions. *Inorganica Chim. Acta* **2015**, *438*, 255–263.

(60) Trose, M.; Dell'Acqua, M.; Pedrazzini, T.; Pirovano, V.; Gallo, E.; Rossi, E.; Caselli, A.; Abbiati, G. [Silver(I)(Pyridine-Containing Ligand)] Complexes as Unusual Catalysts for A3-Coupling Reactions. *J. Org. Chem.* **2014**, *79*, 7311–7320.

(61) Zhao, Y.; Chen, K.; Fan, J.; Okamura, T.; Lu, Y.; Luo, L.; Sun, W.-Y. Structural Modulation of Silver Complexes and Their Distinctive Catalytic Properties. *Dalton Trans.* **2014**, *43*, 2252–2258.

(62) Hassam, M.; Li, W. S. Copper-Catalyzed Markovnikov Hydration of Alkynes. *Tetrahedron* **2015**, *71*, 2719–2723.

(63) Park, J.; Yeon, J.; Lee, P. H.; Lee, K. Iron-Catalyzed Indirect Hydration of Alkynes in Presence of Methanesulfonic Acid. *Tetrahedron Lett.* **2013**, *54*, 4414–4417.

(64) Mainkar, P.; Chippala, V.; Chegondi, R.; Chandrasekhar, S. Ruthenium(II)-Catalyzed Hydration of Terminal Alkynes in PEG-400. *Synlett* **2016**, *27*, 1969–1972.

(65) Li, F.; Wang, N.; Lu, L.; Zhu, G. Regioselective Hydration of Terminal Alkynes Catalyzed by a Neutral Gold(I) Complex [(IPr)AuCl] and One-Pot Synthesis of Optically Active Secondary Alcohols from Terminal Alkynes by the Combination of [(IPr)AuCl] and Cp∗RhCl[(R, R)-TsDPEN]. *J. Org. Chem.* **2015**, *80*, 3538–3546.

(66) Almássy, A.; Nagy, C. E.; Bényei, A. C.; Joó, F. Novel Sulfonated N-Heterocyclic Carbene Gold(I) Complexes: Homogeneous Gold Catalysis for the Hydration of Terminal Alkynes in Aqueous Media. *Organometallics* **2010**, *29*, 2484–2490.

(67) Velegraki, G.; Stratakis, M. Aryl-Substituted Cyclopropyl Acetylenes as Sensitive Mechanistic Probes in the Gold-Catalyzed Hydration of Alkynes. Comparison to the Ag(I)-, Hg(II)-, and Fe(III)-Catalyzed Processes. *J. Org. Chem.* **2013**, *78*, 8880–8884.

(68) Marion, N.; Ramón, R. S.; Nolan, S. P. [(NHC)Au I]-Catalyzed Acid-Free Alkyne Hydration at Part-per-Million Catalyst Loadings. *J. Am. Chem. Soc.* **2009**, *131*, 448–449.

(69) Thuong, M. B. T.; Mann, A.; Wagner, A. Mild Chemo-Selective Hydration of Terminal Alkynes Catalysed by AgSbF6. *Chem. Commun.* **2012**, *48*, 434–436.

(70) Chen, Z. W.; Ye, D. N.; Qian, Y. P.; Ye, M.; Liu, L. X. Highly Efficient AgBF4-Catalyzed Synthesis of Methyl Ketones from Terminal Alkynes. *Tetrahedron* **2013**, *69*, 6116–6120.

(71) Das, R.; Chakraborty, D. AgOTf Catalyzed Hydration of Terminal Alkynes. *Appl. Organomet. Chem.* **2012**, *26*, 722–726.

(72) Venkateswara Rao, K. T.; Sai Prasad, P. S.; Lingaiah, N. Solvent-Free Hydration of

Alkynes over a Heterogeneous Silver Exchanged Silicotungstic Acid Catalyst. *Green Chem.* **2012**, *14*, 1507.

(73) Coles, S. J.; Gale, P. A. Changing and Challenging Times for Service Crystallography. *Chem. Sci.* **2012**, *3*, 683–689.

(74) Dolomanov, O. V; Blake, A. J.; Champness, N. R.; Schröder, M. OLEX: New Software for Visualization and Analysis of Extended Crystal Structures. *J. Appl. Crystallogr.* **2003**, *36*, 1283–1284.

(75) Sheldrick, G. M. SHELXT – Integrated Space-Group and Crystal-Structure Determination. *Acta Crystallogr. Sect. A Found. Adv.* **2015**, *71*, 3–8.

(76) Sheldrick, G. M. A Short History of SHELX. *Acta Crystallogr. Sect. A* **2008**, *64*, 112–122.

(77) Farrugia, L. J. Suite for Small-Molecule Single-Crystal Crystallography. *J. Appl. Crystallogr.* **1999**, *32*, 837–838.

(78) Spek, A. L. Single-Crystal Structure Validation with the Program PLATON. *J. Appl. Crystallogr.* **2003**, *36*, 7–13.

(79) Macrae, C. F.; Edgington, P. R.; McCabe, P.; Pidcock, E.; Shields, G. P.; Taylor, R.; Towler, M.; Van De Streek, J. Mercury: Visualization and Analysis of Crystal Structures. *J. Appl. Crystallogr.* **2006**, *39*, 453–457.

(80) Janiak, C. A Critical Account on Pi-Pi Stacking in Metal Complexes with Aromatic Nitrogen-Containing Ligands. *J. Chem. Soc. Trans.* **2000**, 3885–3896.

(81) Addison, A. W.; Rao, T. N.; Reedijk, J.; Van Rijn, J.; Verschoor, G. C. Synthesis, Structure, and Spectroscopic Properties of Copper(II) Compounds Containing Nitrogen-Sulphur Donor Ligands; the Crystal and Molecular Structure of Aqua[1,7-Bis(N-Methylbenzimidazol-2′;-Yl)-2,6-Dithiaheptane]Copper(II) Perchlorate. *J. Chem. Soc. Dalton Trans.* **1984**, 1349–1356.

(82) Caballero, A. B.; Maclaren, J. K.; Rodríguez-Diéguez, A.; Vidal, I.; Dobado, J. A.; Salas, J. M.; Janiak, C. Dinuclear Silver(I) Complexes for the Design of Metal-Ligand Networks Based on Triazolopyrimidines. *Dalton Trans.* **2011**, *40*, 11845–11855.

(83) Elguero, J.; Katritzky, A. R.; Denisko, O. V. Prototropic Tautomerism of Heterocycles: Heteroaromatic Tautomerism - General Overview and Methodology. *Advances in Heterocyclic Chemistry*. **2000**, 1–84.

(84) Minkin, V. I.; Garnovskii, A. D.; Elguero, J.; Katritzky, A. R.; Denisko, O. V. The Tautomerism of Heterocycles: Five-Membered Rings with Two or More Heteroatoms. *Advances in Heterocyclic Chemistry*. **2000**, 157–323.

(85) Wofford, D. S.; Forkey, D. M.; Russell, J. G. 15N NMR Spectroscopy: Prototropic Tautomerism of Azoles. *J. Org. Chem.* **1982**, *47*, 5132–5137.

(86) Larina, L. I.; Milata, V. 1H, 13C and 15N NMR Spectroscopy and Tautomerism of Nitrobenzotriazoles. *Magn. Reson. Chem.* **2009**, *47*, 142–148.

(87) Schilf, W.; Stefaniak, L.; Witanowski, M.; Webb, G. A. 15N NMR Studies of the Tautomeric Equilibrium of Some 1-Hydroxybenzotriazoles. *Magn. Reson. Chem.* **1985**, *23*, 181–184.

(88) Katritzky, A. R.; Lan, X.; Fan, W.-Q. Benzotriazole as a Synthetic Auxiliary: Benzotriazolylalkylations and Benzotriazole-Mediated Heteroalkylation. *Synthesis (Stuttg).* **1994**, *1994*, 445–456.

(89) Katritzky, A. R.; Rogovoy, B. V. Benzotriazole: An Ideal Synthetic Auxiliary. *Chem. Eur. J.* **2003**, *9*, 4586–4593.

(90) Toma, H. E.; Giesbrecht, E.; Espinoza Rojas, R. L. Spectroscopic and Electrochemical Studies on Linkage Isomerism in Iron(II) Complexes of Benzotriazole, a Corrosion Inhibitor. *Can. J. Chem.* **1983**, *61*, 2520–2525.

(91) Toma, H. E.; Giesbrecht, E.; Rojas, R. L. E. Linkage Isomerism in Penta-

Ammineruthenium(II),(III) Complexes of Benzotriazole. *J. Chem. Soc. Dalt. Trans.* **1985**, 2469–2472.

(92) Rocha, R. C.; Araki, K.; Toma, H. E.; Quõâmica, I. De; Paulo, U. D. S.; Postal, C.; Paulo, S. Linkage Isomerism, Kinetics and Electrochemistry of Ruthenium- Edta Complexes of Benzotriazole. *Transit. Met. Chem.* **1998**, *16*, 13–16.

(93) Rocha, R. C.; Toma, H. E. Linkage Isomerism and Redox Properties of Ruthenium-Polypyridine Benzotriazole Complexes. *Transit. Met. Chem.* **2003**, *28*, 43–50.

(94) Kostakis, G. E.; Xydias, P.; Nordlander, E.; Plakatouras, J. C. The First Structural Determination of a Copper (II) Complex Containing the Ligand [1-(4-((1H-Benzo[d][1,2,3]Triazol-2(3H)-Yl)Methyl)Benzyl)-1H-Benzo[d][1,2,3]Triazole]. *Inorg. Chim. Acta* **2012**, *383*, 327–331.

(95) Tomás, F.; Abboud, J. L. M.; Laynez, J.; Notario, R.; Santos, L.; Nilsson, S. O.; Catalán, J.; Claramunt, R. M.; Elguero, J. Tautomerism and Aromaticity in 1,2,3-Triazoles: The Case of Benzotriazole. *J. Am. Chem. Soc.* **1989**, *111*, 7348–7353.

(96) Katritzky, A. R.; Yannakopoulou, K.; Anders, E.; Stevens, J.; Szafran, M. Ab Initio and Semiempirical Calculations on the Tautomeric Equilibria of N-Unsubstituted and N-Substituted Benzotriazoles. *J. Org. Chem.* **1990**, *55*, 5683–5687.

(97) Dehaen, W. (Wim); Bakulev, V. A. *Chemistry of 1,2,3-Triazoles*; Dehaen, W., Bakulev, V. A., Eds.; Springer International Publishing, 2015.

(98) Katritzky, A. R.; Lan, X.; Yang, J. Z.; Denisko, O. V. Properties and Synthetic Utility of N-Substituted Benzotriazoles. *Chem. Rev.* **1998**, *98*, 409–548.

(99) Katritzky, A. R.; Perumal, S.; Fan, W.-Q. Studies on the Thermal Isomerization of N-Arylmethylbenzotriazoles. *J. Chem. Soc. Perkin Trans. 2* **1990**, 2059–2062.

(100) Smith, J. R. L.; Sadd, J. S. Isomerism of 1- and 2-(NN-Disubstituted Aminomethyl)Benzotriazoles; an Investigation by Nuclear Magnetic Resonance

Spectroscopy. *J. Chem. Soc. Perkin Trans. 1* **1975**, 1181–1184.

(101) Katritzky, A. R.; Yannakopoulou, K.; Kuzmierkiewicz, W.; Aurrecoechea, J. M.; Palenik, G. J.; Koziol, A. E.; Szczesniak, M. The Chemistry of N-Substituted Benzotriazoles. Part 7. Thr Isomeric Composition and Mechanism of Interconversion of Some N-(Aminomethyl)Benzotriazole Derivatives. *J. Chem. Soc. Perkin Trans. I* **1987**, 2673–2679.

(102) Katritzky, A. R.; Rachwal, S.; Rachwal, B.; Steel, P. J. Additions of 1-(α-Aminoalkyl)Benzotriazoles to Enol Ethers. New Routes to 1,3-Amino Ethers. *J. Org. Chem.* **1992**, *57*, 4932–4939.

(103) Katritzky, A. R.; Kuzmierkiewic, W.; Perumal, S. Isomerization of N-[A-(Alkylthio)Alkyl]- and N-[A-(Arylthio)Alkyl]Benzotriazoles. *Helv. Chim. Acta* **1991**, *74*, 1936–1940.

(104) O'Keefe, B. J.; Steel, P. J. Self-Assembly and X-Ray Structure of a Triple Helicate with Two Trigonal Silver(I) Termini. *Inorg. Chem. Commun.* **2000**, *3*, 473–475.

(105) Prat, D.; Hayler, J.; Wells, A. A Survey of Solvent Selection Guides. *Green Chem.* **2014**, *16*, 4546–4551.

(106) Chen, M. T.; Landers, B.; Navarro, O. Well-Defined (N-Heterocyclic Carbene)-Ag(i) Complexes as Catalysts for A 3 Reactions. *Org. Biomol. Chem.* **2012**, *10*, 2206–2208.

(107) Gatto, M.; Belanzoni, P.; Belpassi, L.; Biasiolo, L.; Del Zotto, A.; Tarantelli, F.; Zuccaccia, D. Solvent-, Silver-, and Acid-Free NHC-Au-X Catalyzed Hydration of Alkynes. The Pivotal Role of the Counterion. *ACS Catal.* **2016**, *6*, 7363–7376.

For Table of Contents Use Only

Structural diversity and catalytic properties in a family of Ag(I)-benzotriazole based coordination compounds

Edward Loukopoulos,[a] Alaa Abdul-Sada,[a] Eddy M. E. Viseux,[a] Ioannis N. Lykakis*[b] and George E. Kostakis*[a]

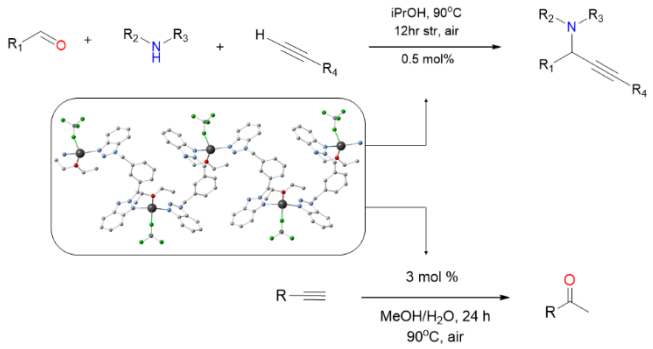

The use of a family of semi-rigid benzotriazole-based ligands and silver salts affords a large structural variety depending on synthetic parameters and ligand selection. A one-dimensional coordination polymer is identified as a suitable homogeneous catalyst for the multicomponent A^3 coupling reaction and the hydration of alkynes, generating high yields under mild conditions.